Oxygen limitation is not a major physiological mechanism restricting early life development in zebrafish

Lorena Silva-Garay[1,*], Moa Metz[1], Henning H. Kristiansen[1], Leon Pfeufer[2], Emily R. Lechner[2], Rasmus Ern[1], Anna H. Andreassen[1,3], Fredrik Jutfelt[1,2]

[1]Department of Biology, Norwegian University of Science and Technology, Trondheim, Norway.
[2]Department of Biological and Environmental Sciences, Faculty of Science, University of Gothenburg, Gothenburg, 413 90, Sweden.
[3]DTU Aqua: National Institute of Aquatic Resources, Technical University of Denmark, Kgs. Lyngby, Denmark

*Corresponding author. Email: lorena.silvagaray@gmail.com (LSG)

Keywords: hypoxia, hyperoxia, embryonic development, oxygen limitation, developmental plasticity.

Abstract

Early life stages are considered particularly vulnerable to warming because tissue oxygen supply is thought to become limiting, given their underdeveloped gill function and reliance on passive oxygen diffusion. Here, we tested whether oxygen availability constrains early development under warming in zebrafish (*Danio rerio*). We exposed embryos and early-stage larvae to a high-resolution factorial design spanning 50 combinations of temperature and oxygen levels, and quantified multiple developmental and physiological responses (including growth- and survival-related performance) as well as carry-over effects on juvenile warming tolerance. Across traits, embryonic and larval performance was less restricted by oxygen availability than expected. Moderate hypoxia did not impair performance across a wide thermal range, while hyperoxia did not rescue performance under warming, indicating that thermal failure was not alleviated by additional oxygen. Developmental failure occurred primarily under the combined effects of severe hypoxia and extreme warming. Severe hypoxia also induced developmental slowing and premature hatching, especially near thermal extremes. Juvenile warming tolerance was reduced by severe hypoxia and extreme developmental temperatures, but the small effect sizes indicate limited carryover effects of developmental plasticity. Together, these findings do not support oxygen limitation as a primary mechanism limiting early-life performance under warming, refining mechanistic expectations of how warming constrains fish performance.

Introduction

Climate change and eutrophication can alter aquatic environments in many ways, including increasing water temperatures and reducing water oxygen levels. These changes can pose strong physiological challenges for aquatic ectotherms, such as fish, whose thermal tolerance windows and geographic distribution are strongly influenced by water temperature and oxygen availability (Sunday et al., 2012; Comte and Olden, 2017). Ectothermic organisms experience temperature-dependent increases in metabolic rate during warming, which elevate their oxygen demand (Fry and Hart, 1948). The oxygen- and capacity-limited thermal tolerance (OCLTT) hypothesis proposes that aerobic performance is constrained at high temperatures when oxygen transport can no longer meet the rising metabolic demand for standard metabolism (Pörtner, 2010; Pörtner et al., 2017). Evidence for a link between thermal performance and oxygen limitation, however, varies among species and life stages (Ern et al., 2016, 2017; Silva-Garay et al., 2025; Andreassen et al., 2022; McArley et al., 2022; Raby et al., 2025), with most research focusing on juvenile and adult stages. A recent meta-analysis suggested that due to oxygen limitation, fish embryos have narrower thermal windows than larvae and adults (Dahlke et al., 2020), creating a developmental bottleneck under climate change. However, this analysis relies partly on imputed thermal tolerance data due to gaps in the available literature and is influenced by methodological differences among studies (Pottier et al., 2022; Cowan et al., 2023). As a result, further research is needed to clarify the role of oxygen availability during warming in early life stages (Du and Shine , 2022; Pottier et al., 2022; Cowan et al., 2024).

Fish embryos face respiratory constraints distinct from those of juveniles and adults. Elevated temperatures accelerate metabolism, increasing oxygen demand and developmental rates, which can compromise the completion of essential developmental milestones (Kamler, 1994; Barrionuevo and Burggren, 1999). These vulnerabilities may be amplified by underdeveloped respiratory and circulatory systems, and by limited or absent behavioral capacity to escape environmental extremes (Warkentin, 2007). Unlike later life stages that rely on active ventilation, embryos obtain oxygen primarily through passive diffusion across the chorion, perivitelline fluid, and embryonic tissues including the yolk sac membrane, which can act as additional diffusion barriers (Hayes et al., 1951; Rombough, 1989; Warkentin, 2007). After hatching, larvae still rely largely on cutaneous diffusion, as their gills and circulatory systems develop (De Silva, 1974; Wells and Pinder, 1996; Rombough, 1999). Although embryos can initially tolerate low water oxygen levels well, their oxygen requirements generally increase throughout development. It has been suggested that oxygen requirements peak close to hatching when the surrounding egg envelope may become a critical barrier to oxygen diffusion (Rombough, 1989; Czerkies et al., 2001). This diffusion-dependent oxygen uptake could thus create a physiological bottleneck that limits the embryos' ability to meet rising metabolic demands under warming or hypoxic conditions (Hassell et al., 2008). As a result, embryonic development may become oxygen-limited, with severity and duration varying among species and environmental conditions.

Embryos can hatch prematurely in response to external stressors, such as warming and hypoxia, a strategy that can come at the cost of underdeveloped physiological and behavioral functions (Alderdice et al., 1958; Keckeis et al., 1996; Wood et al., 2019). Premature hatching may optimize fitness by balancing the trade-offs of remaining within the protective chorion and emerging as a free-swimming larva, but can also be a maladaptive consequence of a stressor (Cowan et al., 2024; Warkentin, 2011). Despite this flexibility, environmental stressors can still impose substantial developmental constraints (Cowan et al., 2024). Both

elevated temperatures and low water oxygen levels impair yolk conversion efficiency, reducing the energy available for growth and organogenesis (Kamler, 1994; Kamiński et al., 2006). Prolonged or severe hypoxia during embryogenesis can lower metabolic rates, delay organ development, and reduce growth, often resulting in reduced hatching success and the emergence of smaller or malformed larvae (Miller et al., 2008; Garside, 1966, Czerkies et al., 2001). While high temperatures and aquatic hypoxia can restrict development by reducing oxygen supply relative to demand, the effects of hyperoxia are still poorly understood. Because hyperoxia can increase tissue oxygen supply capacity in fish (Skeeles et al., 2022) and may enhance oxygen diffusion across the embryonic and larval respiratory surfaces, it has the potential to alleviate oxygen-limitation at high temperatures, when metabolic demand is greatest.

Many studies have explored the effects of water temperature or oxygen on fish early development in isolation (Kamiński et al., 2006; Hassell et al., 2008; Schnur et al., 2014; Negrete et al., 2024), yet few have examined their interactive impacts, despite the fact that these environmental stressors often co-occur in nature. This study investigates whether and how combinations of temperature and oxygen availability during embryogenic development influence developmental performance in wild-caught zebrafish (*Danio rerio*). Zebrafish inhabit subtropical freshwater habitats in South Asia, where diel oxygen fluctuations and episodic heatwaves are common. Although their embryonic development under normoxic, optimal conditions (~28.5 °C) is well characterized (Kimmel et al., 1995), environmental stressors can have major physiological impacts. Previous work has shown that adult zebrafish upper thermal tolerance limits are unaffected by water oxygen across moderate hypoxia to hyperoxia, regardless of acclimation history (Silva-Garay et al., 2025). However, zebrafish larvae thermal tolerance can be constrained by oxygen availability, due to oxygen-limited brain function (Andreassen et al., 2022), suggesting heightened oxygen sensitivity early in development.

To test whether early fish development is constrained by oxygen availability under warming, we exposed zebrafish embryos to a matrix of 50 temperature-oxygen combinations and quantified developmental rate, heart rate, yolk sac depletion, hatching success, larval growth, and survival to first feeding. We also measured juvenile critical thermal maximum (CT_{max}) in fish reared from these embryos to assess developmental carryover effects. Under an oxygen-limitation framework, hypoxia was expected to exacerbate and hyperoxia to alleviate temperature effects if development is oxygen limited. Understanding how oxygen availability constrains early development under warming is essential for improving predictions of fish vulnerability to climate change.

Materials and methods

Study Species and Embryo Collection

The zebrafish (*Danio rerio*) used in this study originated from a wild population collected in 2016 in West Bengal, India (Morgan et al., 2019; Sundin et al., 2019), kept in freshwater aquaria at the Animal Facility of the Norwegian University of Science and Technology (NTNU), Trondheim, Norway. Two independent breeding groups were used to produce embryos for two separate experiments conducted in April (*Experiment 1*) and September (*Experiment 2*), 2024. Parental fish were kept in well-aerated freshwater at 28 °C under a

14:10 h light:dark cycle and fed dry flakes (TetraPro, Tetra Sales, USA) three times daily prior to breeding. In Experiment 1, 42 adults were used for breeding, while 110 were used in Experiment 2. Embryos were collected soon after fertilization, photographed, and identified between the one-cell (0 hours post-fertilization, hpf) and the cleavage stage (~ ¾ to 2¼ hpf) following Kimmel et al. (1995).

From each breeding group, a randomly mixed subset of embryos was used for the experiment. In *Experiment 1*, 750 embryos were distributed across 50 beakers (15 embryos per beaker), and in *Experiment 2*, 1250 embryos were distributed in the same number of beakers (25 embryos per beaker). Each beaker was covered with a plastic lid, secured with a rubberband, and fitted with a small puncture allowing an air tube (PE200; 1.4 mm ID) to supply continuous aeration and mixing. Embryos were kept under the same 14:10 h light:dark photoperiod as the parental fish, and no food was provided during embryonic development or early hatching. All procedures were approved by the Norwegian Food Safety Authority (permit number 8578).

Experimental Setup

Thermal Gradient Table

An aluminum thermal gradient table was used to expose zebrafish embryos to 50 simultaneous unique combinations of temperature and oxygen during their embryonic development and early larval stages. The thermal gradient table was customized after the general design by Thomas et al. (1963) and consisted of a thick aluminium slab with 50 wells, and the dimensions were 122.2 x 53.8 x 17 cm (Thomas et al., 1963; Myrvold , 2020; Haugen , 2022). The table accommodated 50 glass beakers (800 mL) in tightly fitting wells. The layout was a 10 x 5 grid, with each of the 10 rows corresponding to a distinct temperature treatment (Fig. 1A, Fig. S15-S18). A stable linear thermal gradient was generated by heating and cooling opposite ends of the solid aluminum table. The system consisted of a cooler (Titan 200, Aqua Medic, Germany) and a heater circulator (Grant Instruments, GD100), each with a built-in thermostats that maintain their respective water baths at a set temperature. Water from each bath was pumped to the respective edges of the table using an Eheim Universal 1000 pump (Germany), generating a consistent thermal gradient, from cold to warm, across the aluminium slab of the table (Fig. 1B).

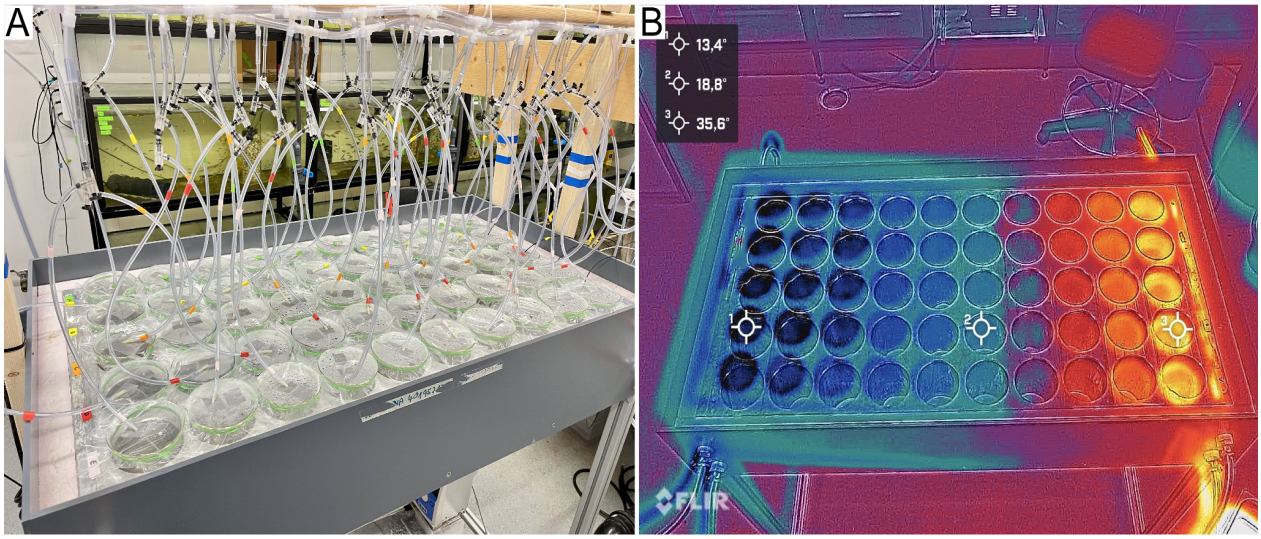

Fig. 1: The aluminum thermal gradient table with 50 different treatment combinations. **(A)** Aluminum gradient table providing 10 temperature treatments and gas mixing lines delivering five oxygen treatments (12.5, 25, 50, 100, and 200% air saturation). **(B)** Thermal image of the gradient surface captured with a FLIR One Pro (Teledyne FLIR LLC).

Oxygen Treatments

Five water oxygen levels (12.5, 25, 50, 100, and 200% air saturation) were maintained by supplying each column of the thermal gradient table with a distinct gas mixture via five independent air lines. Oxygen concentrations were regulated using manual gas flow controllers (RS Pro, 500 ml/min) that mixed air with either nitrogen (50 L, 99.6% N_2) to achieve hypoxia or oxygen (50 L, 99.5% O_2, Linde Co.) to create hyperoxia (Fig. S17). Normoxia was achieved using ambient air. For each oxygen treatment, two flow controllers were used: one for air and one for either nitrogen or oxygen, allowing precise calibration of the gas mixture. The mixed gas was delivered to the respective column of 10 beakers via a 10 mm diameter outflow tube. Each beaker was aerated through an individual air tube tightly inserted through the lid and fitted with an air valve, providing gentle bubbling. This setup ensured homogenous oxygen distribution, minimized gas loss, and maintained consistent aeration and mixing. The order of the oxygen treatments was randomly assigned across the five columns of the gradient table (i.e., *Experiment 1*: 100, 12.5, 25, 200, and 50 % air sat.; *Experiment 2*: 25, 200, 12.5, 50, and 100 % air sat.) Throughout the experimental period, dissolved oxygen (DO_2) concentrations were continuously monitored in each oxygen treatment at the warmest end of the gradient table using fiber-optic oxygen sensor probes (Fig. S2). Additionally, DO_2 and temperature were manually measured in all beakers twice daily between sampling events using optode sensors and a temperature probe (FireStingO_2, PyroScience GmbH).

Experimental Protocol

Experiment 1 - Wide thermal range

Experiment 1 (April 2024) examined embryo development and hatching success across a wide thermal gradient (15.7-39.3 °C: 15.7, 18.1, 20.3, 22.5, 25.2, 27.3, 29.4, 32.0, 35.6, and 39.3 °C) at five oxygen conditions (12.5, 25, 50, 100, and 200% air saturation). Using a plastic pipette, embryos (15-16 per beaker) were gently transferred into sealed glass beakers (800 mL) containing 300 mL of water at 28 °C under normoxic conditions (control). High-resolution images were taken to document the initial developmental stage. Immediately afterwards, the beakers were placed on the gradient table, where temperature and oxygen treatments were applied. Dissolved oxygen levels in the 300 mL water reached target values within ~20 minutes, while target temperatures stabilized within 1-2 hours (with extreme ends of the gradient table requiring the longest to equilibrate). Embryos were photographed approximately every 8 hours (see below for imaging methods). Upon the onset of hatching, a 30-second video of the hatched larvae was recorded. During each sampling event (2-3 min per beaker), lids were removed only briefly (~30 seconds), minimizing disruption to environmental conditions. It was confirmed that temperature and oxygen treatments were only marginally and briefly disturbed by the handling procedure. This experiment continued for 15 days, ending when all surviving embryos had hatched.

Experiment 2 - Upper thermal range

Experiment 2 (September 2024) examined embryo responses to the upper thermal range, using a narrower and warmer gradient (27.8-37.1 °C: 27.8, 28.4, 29.5, 30.4, 31.4, 32.4, 33.3, 34.5, 35.8, and 37.1 °C). Embryos (24-26 per beaker) were processed following the same procedures as in *Experiment 1*. In this experiment, target temperatures were reached within ~1 hour (Fig. S1) and target DO_2 levels after 20 min upon beakers were placed on the gradient table. The embryonic period was documented with video recordings taken every 12 hours (see below for imaging methods). Once hatching began, additional photographs were collected to document the larvae in the beakers. The experiment lasted seven days, concluding when all surviving embryos had hatched.

Dead embryos and larvae were identified based on color changes (e.g., white, cloudy, or opaque appearance) and lack of response to gentle water flow applied via pipette and were removed during observations. Following hatching, larvae remained in their original beakers until just before the transition to exogenous feeding, approximately 2-3 days post-hatching depending on treatment. At that point, a subset of larvae from five temperature treatments across all oxygen levels were transferred to control tanks (28 °C, 100% air saturation) for later assessment of critical thermal maximum (CT_{max}) during the juvenile stage.

Data Collection

Imaging Setup

Two imaging stations were used to capture high-resolution images of embryos and larvae.

Embryo Imaging

Embryos were imaged using a custom-built glass platform with a camera (Sony Alpha 7C, Sony Corp.) and macro lens (Sony FE 2.8/50 Macro, Sony Corp.) mounted below the platform, pointing up. This configuration enabled close-up imaging of embryos resting on the bottom of the beakers, covering an objective area of 40 mm in diameter. A side-mounted LED flood light (133×173×59 mm, 30W, 2400 lumens) positioned 12-15 cm from the focal point enhanced image contrast. In *Experiment 1*, high-resolution photographs (6000×4000 pixels) of embryos were taken (Fig. 2A). In *Experiment 2*, 30-second videos (3840×2160 pixels) were recorded using the same setup (Fig. 2B).

Larval Imaging

Larvae were imaged using a larger LED light platform (470×280×9 mm, Lightcraft Ultraslim A4 Lightbox) placed beneath the beaker for even illumination. A second camera (Sony Alpha 7C) equipped with a macro lens (Sony FE 2.8/90 Macro G OSS) was positioned above the platform pointing downwards, capturing larvae swimming in the water column. Beaker lids were briefly removed (~0.5-1 min) during sampling to prevent changes in air composition. In *Experiment 1*, 30-second videos (1280×720 pixels) of larvae were collected, while in *Experiment 2*, photographs (6000×4000 pixels) were captured.

Data Analysis

Embryo and larval performance were assessed based on a set of fitness-related traits: embryo survival, yolk sac area, and heart rate through the embryonic period, hatching success, larval length at hatch, and survival to the first feeding stage. These metrics were extracted from time-series photo and video analyses.

Yolk Sac Area

Yolk sac surface area (YSA, mm^2) was quantified at three developmental time points starting at 24 hpf, using *ImageJ* software (Abràmoff et al., 2004). For each treatment, five embryos were selected, and two perpendicular yolk sac diameters (length (l) and height (h) in mm) were measured. YSA was estimated using the formula for the area of an ellipse:

$$\text{YSA}=\frac{\pi \cdot l \cdot h}{4}$$

Images were calibrated based on the experimental setup: *Experiment 1*: 390 pixels ≈ 1 mm, *Experiment 2*: 325 pixels ≈ 1 mm.

Thermal performance curves were generated using embryonic yolk consumption, quantified as the percentage reduction in yolk area relative to the average yolk area at 0 hpf for each experiment. Yolk area was subsequently measured at 24, 48, and 72 hpf in *Experiment 1*, and at 24, 36, and 48 hpf in *Experiment 2*. Yolk consumption at each time point was calculated as the proportional decrease in yolk area relative to the initial yolk area using the following formula:

$$\%\ \text{yolk consumed} = \frac{(initial\ yolk\ area - yolk\ area\ at\ time\ t)}{initial\ yolk\ area} \times 100$$

Embryo Heart Rate Measurement

Embryo heart rate was quantified by amplifying subtle pixel-level motion associated with cardiac contractions using Eulerian video magnification (EVM; Lauridsen et al., 2019). This approach enhances small, periodic intensity changes in a video, such as those caused by heartbeats. Videos (1280x720 pixel resolution) were first stabilized in *iMovie* to reduce camera shake by aligning successive frames. Stabilized videos were then processed in Python using the Laplacian pyramid-based motion magnification approach (Burt and Adelson, 1983). This approach enhances very small movements in the video by analyzing the image at multiple spatial scales and gently amplifying motion while reducing noise, making subtle body movements easier to detect. We used a configuration with eight pyramid levels, an amplification strength of 100. Motion signals with spatial wavelengths above 100 pixels were attenuated, and a mild post-filtering step (attenuation factor 0.4 applied to both the I and Q motion channels) was used to reduce noise while preserving biologically relevant movements. The temporary frequency band was restricted to 1.5-3.5 Hz.

To reduce background noise, videos were temporarily cropped around the embryo's heart, typically to a 10x10 pixel region (Fig. S3A). From this region, a vertical scan line (fixed x-coordinate) positioned over the clearest cardiac signal was used to extract a space-time image representing heartbeat dynamics (Fig. S3B). Heart rate was typically extracted from 5-30 s of recording, limited to periods of high image stability with minimal embryo movement. We then applied Fast Fourier Transform with SciPy 1.15.2 to this space-time image to obtain the

frequency spectrum. The dominant peak amplitude within the filtered frequency was considered as the heart rate (Hz) for the analyzed period (Fig. S3C). Frequency values were converted to beats per minute by multiplying by 60. This procedure was applied to up to six embryos per treatment across multiple developmental time points (24-144 hpf) in *Experiment 2*. When background noise prevented reliable frequency detections for six embryos, we analyzed as many individuals as possible.

Survival and Hatching

The number of surviving embryos was determined via visual inspection of embryo color and appearance during samplings and from image recordings throughout the development period. Hatching success ratio was calculated as the proportion of hatched embryos to the total number of fertilized embryos per beaker. Fertilization status was assessed by observing early cleavage stages, such as blastula or blastocyst formation, which became visible at ~24 hours post-fertilization (hpf) in *Experiment 1* and ~12 hpf in *Experiment 2*, depending on temperature and oxygen conditions. In addition, survival to the first feeding stage was defined as the proportion of fertilized embryos per beaker that survived through hatching and reached the exogenous feeding stage, relative to the total number of fertilized embryos. Reaching the first feeding stage was assessed when larvae no longer exhibited a distended yolk sac, indicating near-complete yolk sac absorption, at which point larvae were removed and the treatment was terminated. Larvae displaying severe stress responses, including erratic spiral swimming, tissue swelling, or pronounced spinal deformities, were excluded from survival-to-first-feeding estimates. Exclusions were applied only in cases of clear pathological stress and not to larvae exhibiting delayed but otherwise viable development.

Cumulative larval hatching and embryo survival to first feeding were visualized across temperature and oxygen treatments using 2D plots and 3D surface plots. For the latter, cumulative survival ratios were calculated per treatment and smoothed using a kernel-based normalization (function *image.smoother*, *Fields* package, R Core Team, 2024). This method applies local averaging to the observed data to estimate a continuous surface.

Larval Length at Hatch

Larval total length (TL; measured from head to caudal fin tip in mm) was quantified from all post-hatch images and videos using ImageJ. Image scales were as follows: *Experiment 1*: 7.4 pixels ≈ 1 mm, *Experiment 2*: 35.2 pixels ≈ 1 mm.

CT_{max} Testing

To assess whether developmental plasticity influences heat tolerance later in life, we re-acclimated zebrafish larvae from five developmental temperatures and all oxygen treatments in both experiments to control conditions (28.0 ± 0.5 °C in fish from *Experiment 1* and 27.0 ± 0.5 °C in fish from *Experiment 2*). Surviving larvae were held under control conditions for four weeks (*Experiment 1:* 20.3, 25.2, 29.4, 32.0, 35.6 °C) and six weeks (*Experiment 2:* 27.8, 29.5, 31.4, 33.3, 35.8 °C) prior to critical thermal maximum (CT_{max}) testing. During this reacclimation period, larvae were fed a diet of live artemia and commercial larvae feed (Zebrafeed, Sparos I&D, <100 to 600 µm) three times daily. Upon reaching the juvenile stage (~2-3 weeks post fertilization), fish were transitioned to dry flake diet (TetraPro, Tetra Sales, USA).

CT_{max} is defined as the temperature (°C) at which fish lose equilibrium (LOE) and cannot remain upright for 3 seconds (Morgan et al., 2018). At the point of LOE, fish were immediately removed from the testing arena, and both temperature and time were recorded. The testing protocol followed Morgan et al. (2018). Trials were conducted under control conditions (28 °C and normoxia, 100% air saturation). Groups of 7-9 fish from each rearing condition were transferred from their respective holding tanks to a CT_{max} testing arena (9 liters: 25x22x18 cm). Fish were allowed a 15-minute to condition to the CT_{max} arena before the temperature ramping began. Starting at 28 °C, water temperature was increased at a rate of 0.34 ± 0.02 °C·min^{-1}. Fish were fasted for 16-20 hours before testing. Water in the CT_{max} box was replaced between trials to maintain water quality. To minimize time-of-day and order effects, treatment testing sequences were randomized. CT_{max} trials were conducted within a three-day period for *Experiment 1* and *2*. Following LOE, fish were transferred into an individual recovery tank with water maintained at 28 °C. All individuals recovered equilibrium within 2 min. After a 30-minute recovery period, fish were euthanized via ice immersion, and fish body mass (± 0.01 g), and total length (TL ± 0.1 mm) were recorded.

Fulton's Condition Factor

Using body mass (W) and total length (L) of the fish tested for CT_{max}, we quantified the Fulton Condition Factor (K) as follows:

$$K = \frac{W}{L^3}$$

Statistical Analysis

Physiological Parameters Analysis

We analyzed yolk consumption, heart rate, larval length, CT_{max} and Fulton's condition factor using linear models (LMs) using the *car* package implemented in R (version 4.4.1; R Core Team, 2024). For each response variable, models included oxygen treatment, temperature, and their interaction as fixed effects, together with developmental time (hpf) when appropriate. Temperature was centered to the coldest treatment ($Temp_1$) within each experiment to facilitate interpretation of model coefficients and interaction terms. To capture the non-linearity with respect to temperature of the parameters measured, temperature was added as quadratic ($Temp_2 = Temp_1^2$). Models were constructed as: *Response variable* ~ $Oxygen + Temp_1 + Temp_2 + Oxygen*Temp_1 + Oxygen*Temp_2 + hpf$. For balanced factorial designs, we assessed the significance of predictors using Type II ANOVA, whereas Type III ANOVA was applied when sample sizes were unbalanced or when interaction terms were included. Alternative models were built, removing the quadratic term of temperature, when oxygen or temperature had a linear relationship with the response variable. Models were contrasted using Akaike Information Criterion (AIC) to identify the most parsimonious model structure that best fit the data (*MuMIn* package). We considered a difference of ΔAIC > 2 as evidence of substantial improvement in model fit (Burnham and Anderson, 2004). Estimates, standard errors, and p-values (with significance $p < 0.05$) reported in the Results section derive from these fitted linear models. Model assumptions were evaluated via inspection of residual distributions and homoscedasticity.

Hatching Success Analysis

Hatching probability and larval survival were analyzed using binomial generalized linear models (GLMs, *glm* package; Brooks et al., 2017) with a logit link, fitted using bias-reducing adjusted score estimation (*brglmFit*) to mitigate small-sample and separation issues. Oxygen treatment, temperature, their interaction, and developmental time (log-transformed hours post-fertilization, hpf) were included as fixed effects, with the number of fertilized embryos specified as the binomial denominator. The model was specified as: (*Larval hatched, Initial embryos - Larval hatched*) ~ *Oxygen * Temperature + log(hpf)*. From these models, we estimated the time to 50% hatching (ET_{50}) for each temperature–oxygen combination in both experimental runs by interpolating predicted hatching probabilities from the fitted curves using the functions *predict* and *approx*. Treatment effects were assessed by contrasting model predictions against control conditions (normoxia at 27.3 °C in *Experiment 1* and 27.8 °C in *Experiment 2*).

Because hatching responses exhibited a nonlinear relationship with temperature, an alternative model incorporating a quadratic temperature term was also evaluated, consistent with the modelling approach used for other traits: (*Larval hatched, Initial embryos - Larval hatched*) ~ *Oxygen + Temp$_1$ + Temp$_2$ + Oxygen*Temp$_1$ + Oxygen*Temp$_2$ + log(hpf)*; where Temp1 and Temp2 represent linear and quadratic temperature terms, respectively. This model was used to assess the effect of oxygen on thermal performance of both hatching success and survival to first feeding across temperatures. Model goodness-of-fit was evaluated using residual deviance (residual deviance/degrees of freedom ≈ 1), inspection of diagnostic plots, and examination of predicted probability curves. Statistical significance was assessed at $\alpha = 0.05$. Parameter estimates reported in the Supplementary Materials correspond to log-odds coefficients, along with their standard errors, z-values, and associated p-values derived from the fitted GLMs.

Results

Yolk Sac Area

In *Experiment 1* (15.7 to 39.3 °C), yolk consumption was affected by temperature, oxygen availability, their interaction, and developmental time ($p < 0.001$ all; Fig. 2A-C; Fig. S4A-S5A; Table S1). Under normoxia, yolk utilization increased steeply with warming from the coldest treatment ($Temp_1$: $\beta = 5.01 \pm 0.45$, $p < 0.001$) and declined above 32 °C ($Temp_2$: $\beta = -0.195 \pm 0.020$, $p < 0.001$) forming a thermal performance curve in which embryos at 22.5 - 32 °C consumed yolk fastest. Oxygen availability strongly altered this temperature dependence. At the lowest temperatures, severe hypoxia increased yolk consumption ($\beta = 7.66 \pm 2.88$, $p = 0.008$; $\beta = 6.14 \pm 2.85$, $p = 0.032$), coinciding with delayed early development and developmental arrest at 15.7 °C. Above 20.3 °C, however, hypoxia consistently reduced yolk consumption ($\beta = -10.19 \pm 1.52$, $p < 0.001$ at 12.5%; $\beta = -5.03 \pm 1.51$, $p = 0.001$ at 25%; $\beta = -7.15 \pm 1.54$, $p < 0.001$ at 50%). Severe hypoxia (12.5% and 25% air saturation) markedly reduced the increase in yolk use with warming, flattening and narrowing the thermal performance curve ($O_2 \times Temp_1$: $\beta = -4.39 \pm 0.65$, $t = -6.78$, $p < 0.001$ for 12.5%; $\beta = -2.68 \pm 0.63$, $p < 0.001$ for 25%). Moderate hypoxia also slowed yolk use at warm temperatures ($\beta = -1.34 \pm 0.67$, $p = 0.048$), whereas hyperoxia had no detectable effect relative to normoxia ($\beta = -1.16 \pm 3.29$, $p = 0.47$).

In *Experiment 2* (27.8 - 37.1 °C), yolk sac dynamics mirrored those observed in *Experiment 1* ($p < 0.001$ all; Fig. 2B-D; Fig. S4B-S5B; Table S2). Yolk consumption increased from 27.8 °C ($Temp_1$: $\beta = 2.74 \pm 0.74$, $p < 0.001$) and declined at the highest temperatures ($Temp_2$: $\beta = -0.325 \pm 0.078$, $p < 0.001$). Severe hypoxia (12.5 and 25% air saturation) resulted in reduced yolk consumption across temperatures ($\beta = -21.62 \pm 1.91$, $p < 0.001$ at 12.5%; $\beta = -8.60 \pm 1.91$, $p < 0.001$ at 25%), whereas moderate hypoxia and hyperoxia did not differ from normoxia (Table S2, Fig. 3B). Unlike *Experiment 1*, oxygen and temperature interactions were weak in this warmer range. Hypoxia consistently reduced yolk consumption, only moderate hypoxia showed a detectable change in the temperature effect at high temperatures ($O_2 \times Temp_2$: $\beta = 0.296 \pm 0.110$, $p = 0.007$).

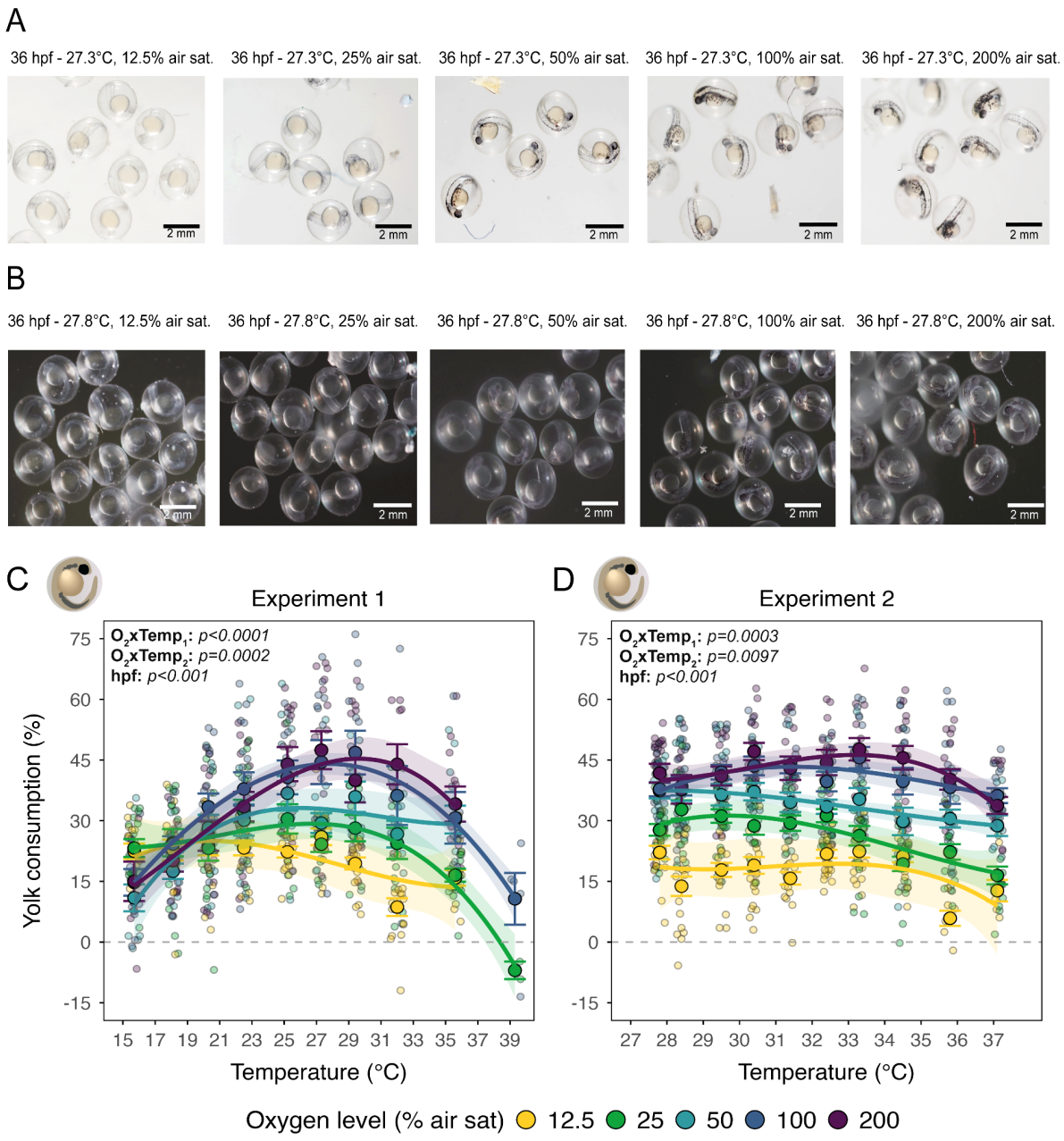

Fig. 2: Yolk consumption (%) of embryos across temperature and oxygen treatments. **(A)** Zebrafish embryonic developmental progress at 36 hpf across oxygen levels at 27.3 °C in *Experiment 1*. **(B)** Equivalent data at 27.8 °C in *Experiment 2*. **(C-D)** Yolk consumption (% of initial yolk area, mm^2) across temperatures (x-axis) and oxygen treatments (colors) in

Experiment 1 (**C**; n = 2–9) and *Experiment 2* (**D**; n = 2–11). Points show individual embryos; circles indicate means ± s.e, lines represent second-degree polynomial fits by oxygen level. P-values are based on Anova (type III; Table S1-S2).

Heart Rate

Experiment 2

Embryonic heart rate exhibited nonlinear temporal dynamics, and was strongly influenced by oxygen availability, temperature, but not their interaction (Fig. 3A-B; Table S3). Centered at 27.8 °C under normoxia, heart rate increased with warming from the coldest treatment ($Temp_1$: $\beta = 19.60 \pm 3.72$, $p < 0.001$) and declined at the warmest temperatures (~>33.3 °C; $Temp_2$: $\beta = -2.19 \pm 0.41$, $p < 0.001$), showing a unimodal thermal response. Heart rate increased steadily over developmental time ($\beta = 1.63 \pm 0.08$, $p < 0.001$) from its onset at ~24 hpf and approaching a plateau prior to hatching. Severe hypoxia (12.5% air saturation) delayed the onset of heart activity and markedly reduced heart rate across temperatures ($\beta = -96.20 \pm 8.72$, $p < 0.001$), while 25% air saturation also lowered heart rates, with stronger effects at warmer temperatures ($\beta = -19.15 \pm 8.91$, $p = 0.032$). Heart rates under 50% and 200% air saturation did not differ from normoxia. Oxygen-temperature interactions were generally weak, indicating that oxygen mainly shifted overall heart rate rather than altering its temperature dependence; only 50% air saturation showed detectable interaction effects ($Temp_1$: $\beta = -12.96 \pm 5.84$, $p = 0.027$; $Temp_2$: $\beta = 1.44 \pm 0.67$, $p = 0.032$). The higher variability in heart rate above 33.3 °C likely reflects measurements from embryos that failed to hatch on time (~48 hpf) and exhibited delayed or abnormal development.

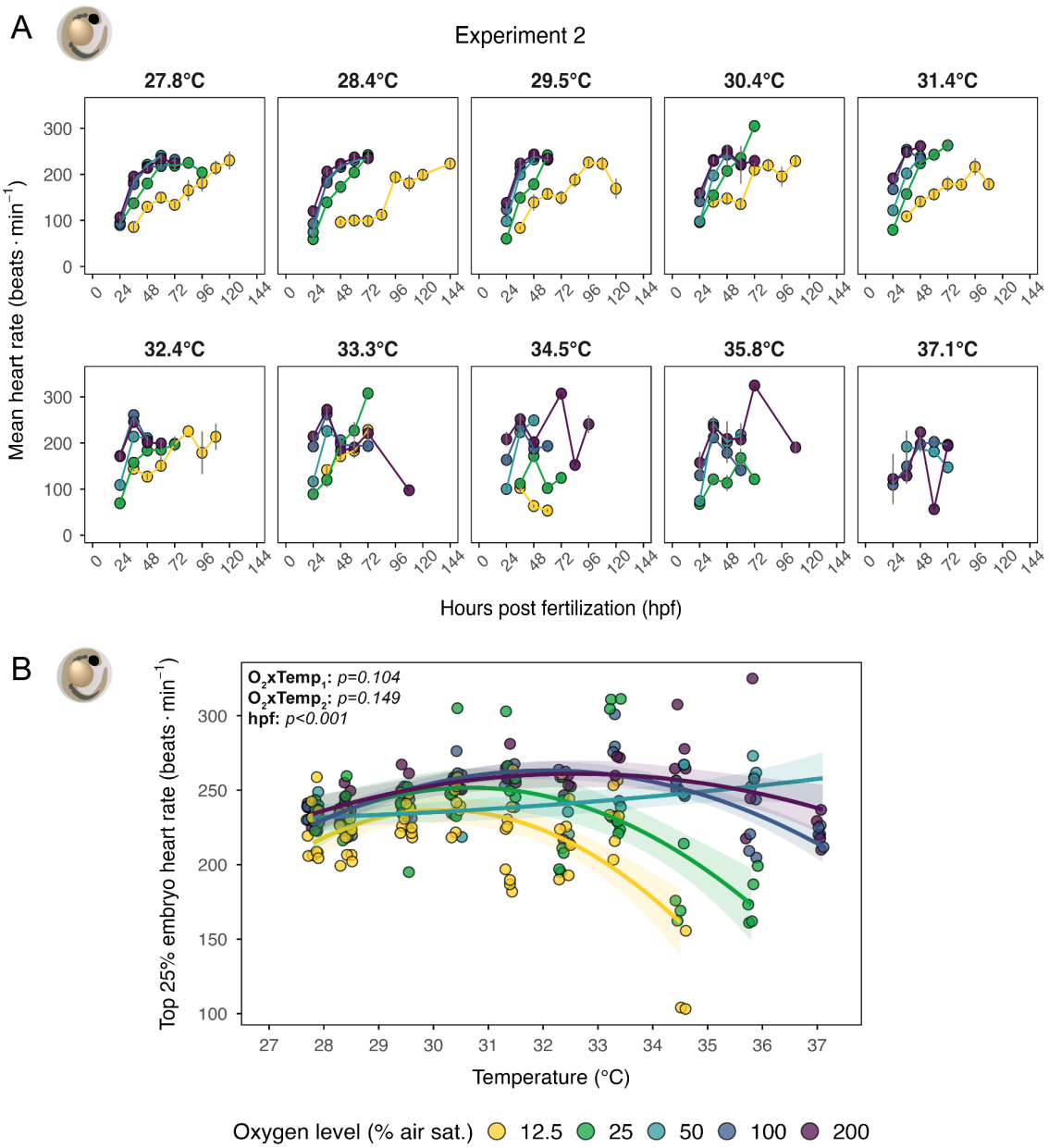

Fig. 3: Embryonic heart rate across temperature and oxygen treatments. **(A)** Mean heart rate (beats min^{-1}) of *Danio rerio* embryos in *Experiment 2* over developmental time, calculated as the average of individual embryo heart rates within each temperature-oxygen treatment (n = 1-8 embryos per time point). Colors indicate oxygen levels. Points show mean ± s.e. **(B)** Top 25th percentile of embryo heart rates (beats min^{-1}) by temperature-oxygen treatment, with percentiles calculated from all measurements pooled across developmental time. Colored points representing individual embryo measurements, lines show second-degree polynomial fits by oxygen level. P-values are based on Anova (type III; Table S3).

Hatching Success

Experiment 1

Across the wide thermal range tested (15.7-39.3 °C), hatching rate was influenced by temperature, oxygen level, their interaction, and developmental time (GLM, all $p < 0.0001$; Fig. 4A; Table S4). Under normoxia, embryos showed a clear thermal window for successful development: hatching was delayed and reduced at 18.1 °C, and increased sharply from 20.3 to 35.6 °C (with >75% hatching across this range), and was fastest near 27.3-32 °C. No hatching occurred at the extreme temperatures, 15.7 °C and 39.3 °C. Oxygen availability strongly modified this thermal response (Fig. 4C; see Fig. S6A-S7A-S8). At 18.1 °C, hatching was delayed and reduced across all oxygen treatments, and especially under hypoxia (≤ 50% air saturation; $p < 0.001$) and hyperoxia (200% air saturation; $p < 0.001$). Severe hypoxia (12.5% air saturation) showed hatching rates comparable to normoxia (~80-100%) between 20.3 and 27.3 °C but rate declined at 29.4 °C (~75%) and ceased at 32.0 °C. Hypoxia (25% air saturation) similarly showed hatching rates comparable to normoxia at cooler temperatures, but lowered hatching to ~75% at 32.0 °C ($p = 0.001$), and suppressed hatching at higher temperatures. Both moderate hypoxia (50%) and hyperoxia (200%) reduced hatching at the warmest temperature (35.6 °C) only, where hatching declined to ~50% (both $p < 0.001$; Table S5).

A GLM including the temperature–oxygen interaction provided the best fit for estimating time to 50% hatch (ET_{50}; Table S5; Fig. S9A). Hatching time decreased steeply with warming, from: ~224-279 hpf at 18.1 °C and 126-200 hpf at 20.3 °C, to 51-79 hpf at 27.3 °C and 41-78 hpf at 32 °C (Table S6). Oxygen availability further modified this temperature dependence. At cooler temperatures (≤ 27.3 °C), severe hypoxia (12.5-25% air saturation) accelerated hatching by ~20-70 h relative to normoxia. In contrast, at warmer temperatures hypoxia progressively delayed hatching by ~25-50 hours, indicating a temperature-dependent shift in the effect of oxygen on developmental timing. Hyperoxia delayed hatching time only at the warmest temperature (35.6 °C).

Experiment 2

Within the warmer developmental range (27.8-37.1 °C), hatching success was again influenced by temperature, oxygen level, their interaction, and developmental time (GLM, all $p < 0.001$; Fig. 4B; Table S6). Under normoxia, hatching remained high (90-100%) from 27.8 to 35.8 °C, and failed entirely at 37.1 °C. Oxygen acted as a major modifier of this thermal window (Fig. 4C; see Fig. S6B-S7B-S8). Severe hypoxia (12.5% air saturation) consistently reduced and delayed hatching across most temperatures ($p < 0.001$), with complete hatching failure at 34.5 °C ($p = 0.0002$; Table S7). Hypoxia (25%) produced hatching rates comparable to normoxia at 27.8-28.4 °C, but reduced hatching at 32.4 and 33.3 °C (both $p < 0.001$) and suppressed hatching at 34.5 °C, consistent with findings from *Experiment 1*. Moderate hypoxia (50%) produced hatching comparable to normoxia, but strongly reduced and delayed hatching at 35.8 °C ($p = 0.001$). Hyperoxia (200%) did not improve hatching success relative to normoxia across this temperature range (27.8-35.8 °C); yet, it reduced the hatching success to a ~50% at 35.8 °C ($p < 0.001$), mirroring the pattern observed in *Experiment 1*.

Consistent with these patterns, the ET_{50} model (GLM; Table S7; Fig. S9B) revealed strong oxygen effects across 27.8-37.1 °C, consistent with patterns observed in *Experiment 1*. Severe hypoxia (12.5% air saturation) markedly delayed hatching through this thermal range, with ET_{50} occurring ~68-136 hpf later than under normoxia (41-62 hpf; Table S6). Hypoxia

(25%) produced ET_{50} estimates comparable to normoxia at the cooler temperatures (~56 hpf at 27.8-28.4 °C), but increasingly delayed hatching at warmer temperatures ($ET_{50} \approx$ 59-80 hpf), mirroring the temperature-dependent shift seen in *Experiment 1*. As in the first experiment, severe hypoxia delayed hatching throughout the upper thermal range (≥27.8 °C) relative to normoxia, contrasting with the earlier hatching observed at lower temperatures. Hyperoxia also delayed the hatching time only at the warmest temperature (35.8 °C).

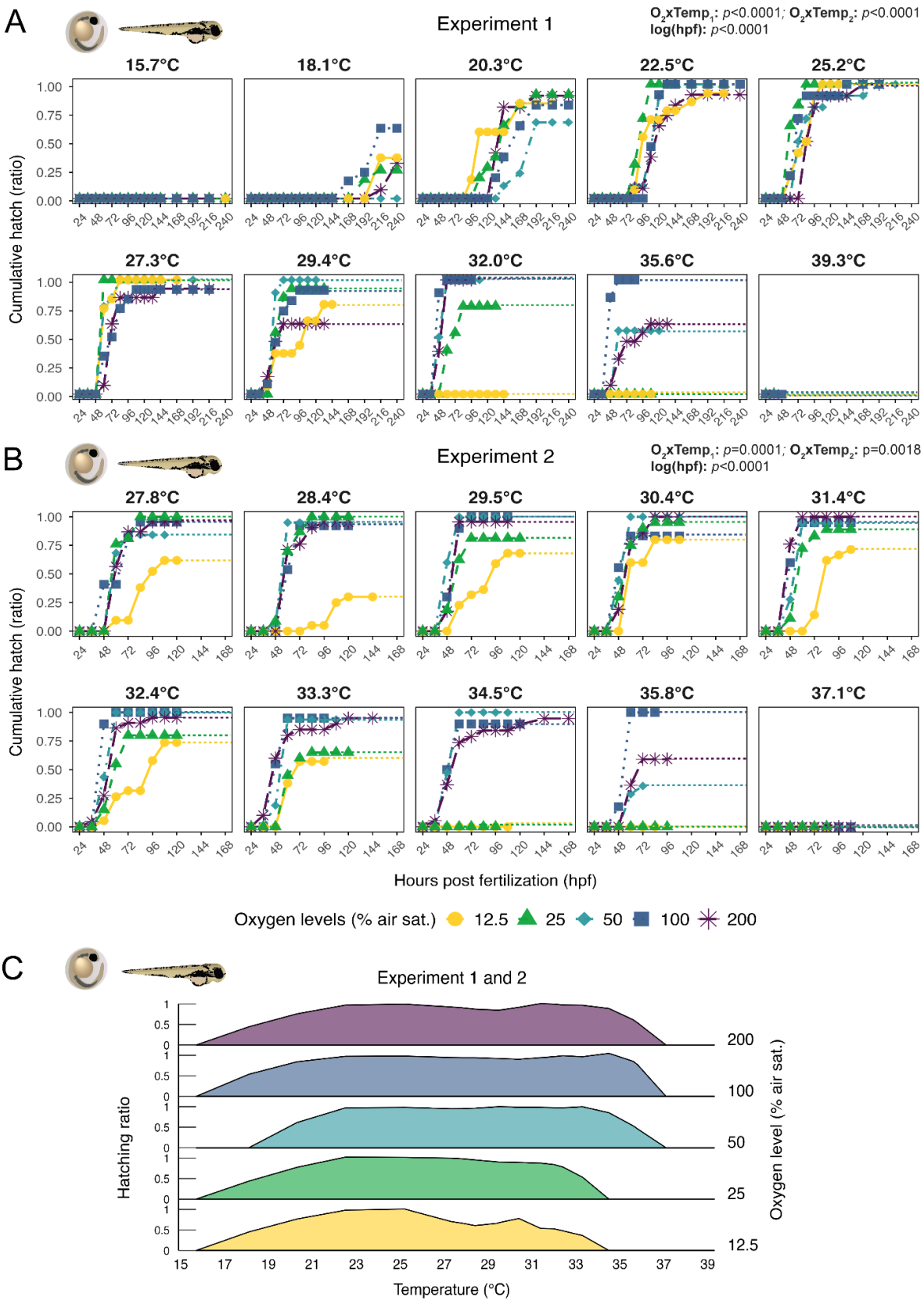

Fig. 4: Hatching dynamics across temperature and oxygen treatments. (A) Cumulative hatching ratio of *Danio rerio* embryos over time (hpf) across temperatures (panels) and oxygen levels (colors) in *Experiment 1* (n = 8-15). **(B)** Equivalent data for *Experiment 2* (n = 13-23). Symbols denote observed hatching ratios; dotted lines indicate periods when larvae

were removed following mortality or completion of hatching. P-values are based on binomial GLM (Table S4-S6). **(C)** Maximum hatching ratio across temperatures combining *Experiment 1* and *Experiment 2*. The ridgeline represents smoothed maxima using a *LOESS* function (span = 0.45).

Larvae Length

In *Experiment 1*, larval length varied with temperature, oxygen availability, and developmental time, but not with the interaction temperature-oxygen ($p < 0.001$; Fig. 5A; Table S9; Fig. S10A-S11). Under normoxia and centered at 18.1 °C, length increased with warming from the coldest treatment ($Temp_1$: $\beta = 0.085 \pm 0.017$, $p < 0.001$) and declined slightly at higher temperatures ($Temp_2$: $\beta = -0.0042 \pm 0.0009$, $p < 0.001$). Severe hypoxia (12.5% air saturation) produced the largest reduction in length across temperatures ($\beta = -0.423 \pm 0.139$, $p = 0.002$), while hyperoxia caused a moderate decrease ($\beta = -0.250 \pm 0.117$, $p = 0.033$). Hypoxia (25% air saturation) reduced length only at temperatures above 22.5 °C ($\beta = -0.145 \pm 0.042$, $p = 0.001$), whereas 50% air saturation did not differ from normoxia. Oxygen-temperature interactions were weak, suggesting that oxygen primarily shifted mean larval length without strongly altering its response to temperature. Length increased modestly with developmental time ($\beta = 0.00094 \pm 0.00025$, $p < 0.001$).

In *Experiment 2*, larval length also varied with oxygen availability and developmental time, but showed no temperature effects ($p < 0.001$; Fig. 5B; Table S10; Fig. S10B-S12). Length was no different across temperatures ($Temp_1$: $p = 0.44$; $Temp_2$: $p = 0.46$). Oxygen availability had a clearer influence: larvae reared in hypoxia were consistently smaller across temperatures, with the strongest reduction at 12.5% ($\beta = -0.410 \pm 0.062$, $p < 0.001$), followed by moderate reduction at 25%, 50%, and 200% air saturation (all $p \leq 0.02$). As in *Experiment 1*, oxygen-temperature interactions were generally weak, and mostly driven by larval length at hyperoxia and 27.8 °C. Larval length also increased modestly with developmental time ($\beta = 0.00445 \pm 0.00042$, $p < 0.001$).

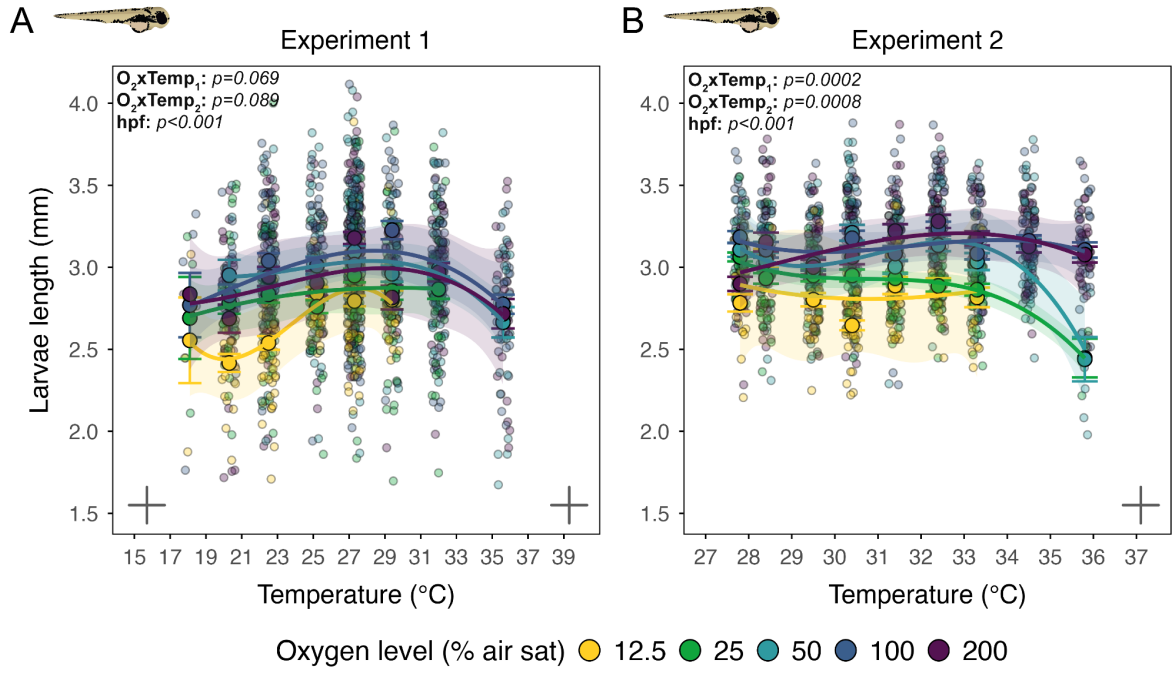

Fig. 5: Larval length across temperature and oxygen treatments. (A) Larval length (mm) of *Danio rerio* across oxygen levels and temperatures in *Experiment 1* (n = 2-15). **(B)** Equivalent data for *Experiment 2* (n = 2-24). Points represent individual larvae; colored circles indicate means ± s.e., lines show third-degree polynomial fits. P-values are based on Anova (type III; Table S9-S10).

Survival To First Feeding Stage

Survival to the first feeding stage showed significant main and interactive effects of temperature and oxygen availability when results from *Experiments 1* and *2* were combined (Fig. 6; Table S11). At 18.1 °C, hatching was substantially delayed (~225-275 hpf), and surviving larvae exhibited retarded development, retaining large yolk sacs for an additional 48-72 h after hatching. Because the experiment was terminated at this point, these individuals were included in estimates of survival to first feeding despite incomplete yolk sac absorption, as they reflected delayed development rather than mortality. In contrast, under extreme warming (~35.6-35.8 °C) and hyperoxia, larvae had consumed the yolk sac but exhibited severe deformities (e.g., spinal malformations or tissue swelling), hence were excluded from survival-to-first-feeding estimates.

Normoxia supported high survival (>80%) across a broad thermal range (~20-35 °C), with mortality increasing towards the warmer extreme (Fig. S8). At lower temperatures, larvae successfully completed endogenous feeding, resulting in high survival to the first feeding stage across all oxygen levels. In contrast, elevated temperatures induced substantial mortality, which increased progressively with the severity of hypoxia (all $p < 0.001$; Table S11). Survival declined below 50% at 34 °C under 50% air saturation, above 32 °C under 25%, and above 27 °C under 12.5%. Notably, extreme heat (~35°C) combined with hyperoxia also markedly reduced survival to first feeding ($p < 0.001$), whereas under normoxia survival closely matched hatching success. The slight valley at intermediate–high temperatures and hyperoxia appears to be an artifact of combining the two experiments rather than a biologically meaningful effect, as survival remained relatively high throughout that range.

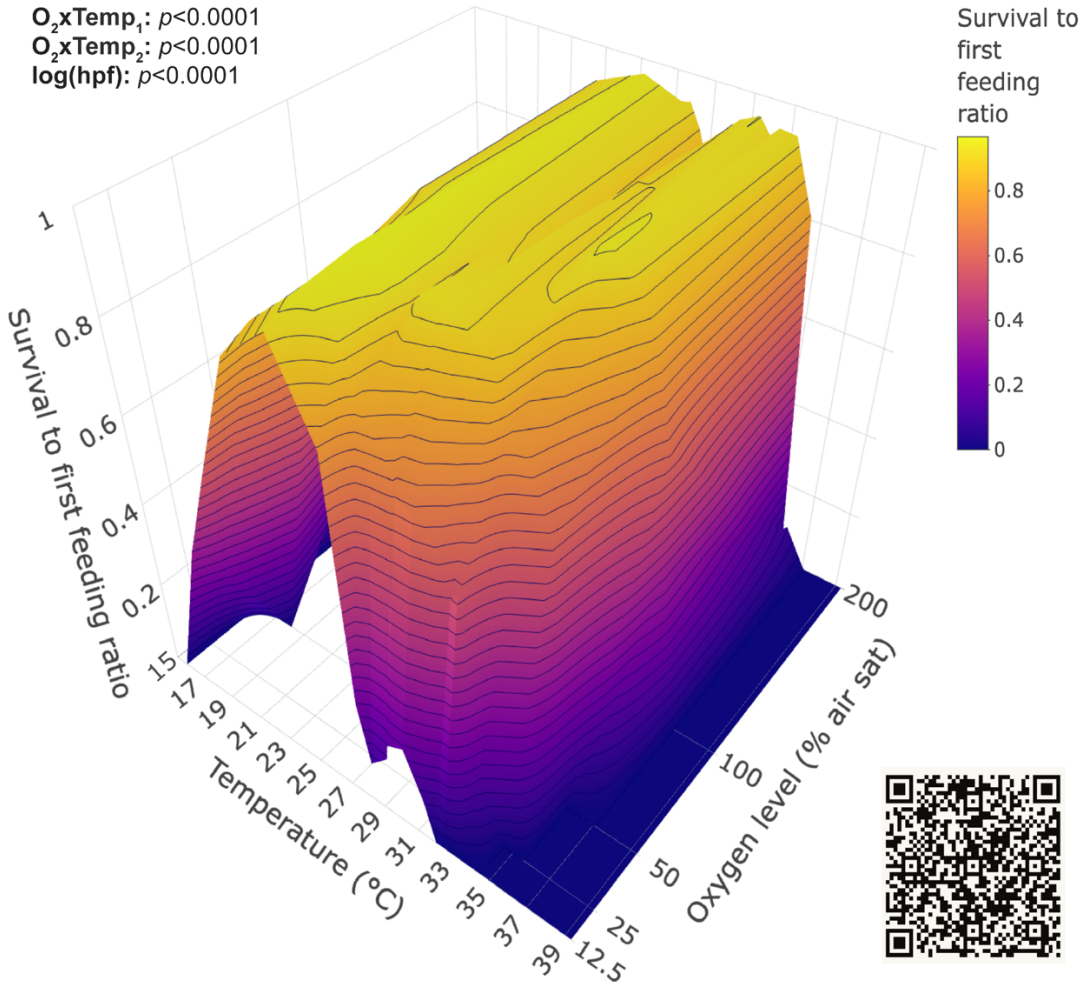

Fig. 6: Three-dimensional surface plot of zebrafish larval survival across temperature and oxygen treatments. 3D surface plot showing the proportion of fertilized *Danio rerio* embryos surviving to first feeding across temperature and oxygen treatments (combined data from *Experiment 1* and *Experiment 2*; 15.7-39.3 °C). Survival ratios above 0.6 were smoothed using a kernel-based normalization (*aRange*, *theta* = 0.9). P-values are based on a binomial GLM-Tmb (Table S11). An interactive version of this figure is available at: [https://loresilvag.github.io/Interactive-3Dplot/3D_SurvivalToFirstFeeding_Plot.html]

Fulton's Condition Factor and CT_{max}

In *Experiment 1*, larvae reared at five temperatures and oxygen levels were re-acclimated to control conditions before CT_{max} testing (Table S12). Larvae hatched at 12.5% air saturation in the warmer treatments died before transfer, and post-transfer mortality regardless of the rearing oxygen level was high at the hottest temperatures, preventing full factorial testing (Fig. S13A). Fulton's condition factor of juvenile fish did not differ across rearing temperatures or oxygen levels (p = 0.076 and p = 0.150, respectively; Table S15, Fig. S14A). CT_{max} varied significantly with rearing temperature (Anova type III: p < 0.001), but not with oxygen or the oxygen-temperature interaction (Fig. 7A; Table S13). Post hoc comparisons centered to normoxia and 20.3 °C showed that early exposure to severe hypoxia (12.5% air saturation) reduced CT_{max} (β = -0.304 ± 0.138, p = 0.031), while 25%, 50%, and 200% air saturation did not differ from normoxia. CT_{max} was also lower in fish reared at 20.3 °C (β = -

0.324 ± 0.122, p = 0.010), unchanged at 25.2 and 32 °C, and marginally reduced at 35.6 °C (β = -0.436 ± 0.222, p = 0.053).

In *Experiment 2*, early mortality under severe hypoxia and warm temperatures similarly limited the number of treatment combinations available for testing. (Fig. S13B). Fulton's condition factor also did not vary across temperatures or oxygen levels (p = 0.387 and p = 0.426, respectively; Table S15, Fig. S14B). CT_{max} varied with both oxygen availability and rearing temperature (Anova type II: both $p < 0.001$), with a border-line interaction (p = 0.056; Fig. 7B, Table S14). Developmental exposure to 25% air saturation reduced CT_{max} (β = -0.483 ± 0.09, $p < 0.001$), same in the 50% air saturation fish (β = -0.158 ± 0.073, p = 0.032), while hyperoxia (200%) did not differ from normoxia. Relative to 27.8 °C, CT_{max} was lower in fish reared at 33.3 °C (β = -0.164 ± 0.082, p = 0.04), while intermediate temperatures produced no difference. Although overall interactions were weak, moderate hypoxia at higher temperatures produced small but detectable reductions in CT_{max} (e.g., at 31.4 °C and 33.3 °C).

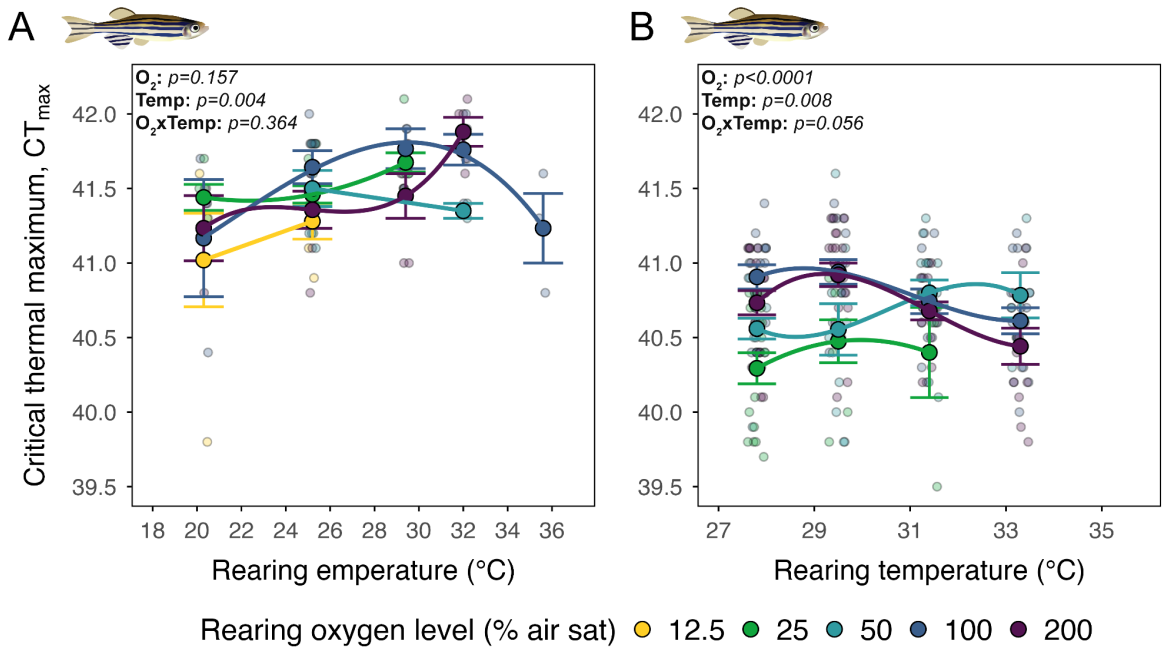

Fig. 7: Critical thermal maximum (CT_{max}) of juvenile zebrafish following early life exposure to temperature and oxygen treatments. (A) CT_{max} of juveniles reared under five oxygen levels (colors) and temperature treatments (panels) in *Experiment 1*. **(B)** Equivalent CT_{max} data for *Experiment 2*. Points represent individual fish (jittered); circles show means ± s.e., and lines depict polynomial fits. P-values are based on Anova (type III; Table S13-S14).

Discussion

Negligible effects of water oxygen availability on embryo development and hatching

By leveraging the many treatment combinations of the thermal gradient table, we examined how the thermal-oxygen landscape influences zebrafish early development. Because embryos

and early larvae rely on passive diffusion of oxygen across the chorion and perivitelline fluid, hyperoxia was hypothesized to buffer against oxygen limitation during thermal stress. We therefore predicted that oxygen availability would play a dominant role in shaping thermal performance, especially at supraoptimal temperatures. Contrary to these predictions, the role of oxygen on developmental performance was relatively minor. Increasing oxygen availability through hyperoxic water did not alleviate key symptoms of thermal stress. Even at the highest temperatures, hyperoxic water did not improve yolk consumption, hatching, or larval growth and survival. This lack of benefit from hyperoxia is consistent with observations in rainbow trout (*Oncorhynchus mykiss*) embryos, where growth was similar under hyperoxia and normoxia rearing (Ciuhandu et al., 2005), and in Atlantic salmon (*Salmo salar)* where hyperoxic rearing (150% air saturation) through embryonic and alevin development did not enhance growth or aerobic metabolism (Wood et al., 2019). Together, these findings indicate that developmental constraints under warming are not readily explained by OCLTT predictions (Dahlke et al., 2020).

Hyperoxia delayed hatching in zebrafish (by 26-50 h), but only at the highest temperatures. Similar delays were reported in rainbow trout (*Oncorhynchus mykiss*) and Atlantic killifish (*Fundulus heteroclitus,* Dimichele and Taylor, 1980; Latham and Just, 1989). As hatching has been hypothesized to be triggered by hypoxia in the embryo (Czerkies et al., 2001; Teletchea and Pauly 2024), hyperoxic water that reduces diffusive constraints across the chorion and perivitelline fluid would accordingly delay hatching, although empirical support for this mechanism remains limited. We only found delayed hatching from hyperoxia at the very highest temperatures, meaning it does not appear to delay hatching in general. The hypothesis is also not supported by our moderate hypoxia groups, where earlier hatching would have been predicted. As this was not found, and because hyperoxia did not delay hatching at most temperatures, we don't see evidence for embryonic oxygen limitation as a universal trigger for hatching.

Similar to the relatively minor effects of hyperoxia, mild hypoxia (50% air saturation) did not dramatically exacerbate the thermal performance of embryos and larvae in most of our measurements. There appeared to be a slight slowing of yolk consumption at higher temperatures, but heart rate, hatching success, and larvae length were mostly unaffected until the very highest temperatures. Taken together, the limited effects of hyperoxia and mild hypoxia suggest that tissue oxygen availability is not a major physiological mechanism restricting development in zebrafish.

Severe hypoxia allows early development but imposes physiological costs

Remarkably, embryos reared under severe hypoxia (12.5 and 25% air saturation) showed high hatching success (60-100%) across a broad thermal range (~20-33 °C), indicating substantial tolerance to low oxygen levels. Yet, severe hypoxia produced clear signs of developmental disturbance, including reduced heart rates, slowed yolk consumption, reduced body length, and delayed and underdeveloped hatching, particularly near thermal limits. These patterns are consistent with hypoxia-induced metabolic depression, a response observed in many teleosts embryos (Shumway et al., 1964; Hassell et al., 2008; Mueller et al., 2011; Marks et al., 2012). Edema and diminished skin pigmentation were also observed in the severe hypoxia-exposed embryos but were not quantified. Notably, embryos exposed to

severe hypoxia exhibited lower heart rates than those reared at higher oxygen levels from the onset of cardiac activity (~24 hpf). Although they eventually reached peak heart rates comparable to those observed in normoxic embryos, this occurred several days later under severe hypoxia. Because this pattern is consistent with observed trajectories of cardiac development in zebrafish (Gierten et al., 2020), it likely reflects delayed or slowed cardiac development rather than persistent bradycardia. While heart rate itself is unlikely to directly constrain aerobic metabolism at this stage due to reliance on diffusive oxygen uptake, delayed cardiac and organ development can nonetheless impair overall performance. Hatching under severe hypoxia is a common and well-documented response in fish embryos exposed to suboptimal environmental conditions, including hypoxia and elevated temperatures (Czerkies et al., 2001; Cowan et al., 2024). Mechanistically, sustained hypoxia during late embryogenesis can trigger the release of chorionase from hatching gland cells, softening the chorion and facilitating earlier escape (Czerkies et al., 2001, 2002). However, if embryos are weakened or hatching glands remain immature, hatching may fail (Czerkies et al., 2001; Mueller et al., 2011). Thus, while stress-induced hatching may enable embryos to exit unfavorable environments, it can occur before completion of key developmental milestones required for post-hatching function.

Despite the developmental stress observed before hatching, survival to the first feeding remained high under severe hypoxia at cooler temperatures (18-27 °C), but declined sharply when hypoxia was combined with supraoptimal temperatures. Similar to embryos, early larvae oxygen transport relies mostly on cutaneous uptake because the gills are not yet functional (De Silva, 1974; Wells and Pinder, 1996). In zebrafish, the neuroepithelial cells that facilitate oxygen uptake begin to develop in the gill filaments at around five days post-fertilization at 28 °C (Jonz and Nurse, 2005). Metabolic demands can rise during this period and cutaneous respiration can thus become insufficient. This may explain why larvae exposed to severe hypoxia and warming showed time-limited survival, and experienced the highest mortality after transfer to normoxia for CT_{max} testing (Fig. S13). By contrast, larvae reared under severe hypoxia and cooler temperatures that were transferred to normoxia for later CT_{max} testing showed high survival rates and reached body sizes comparable with normoxia reared larvae. Together, these results suggest that the early post-hatching transition represents a critical window during which increasing metabolic demands can outpace diffusive oxygen uptake, leaving larvae particularly vulnerable when hypoxia and warming occur simultaneously.

Temperature is a key regulator of fish embryonic development, influencing both yolk utilization and larval growth efficiency (Kamler, 1994; Kamiński et al., 2006). In our study, warmer temperatures predictably accelerated yolk consumption, development and hatching. Furthermore, severe hypoxia had a temperature-dependent and non-linear effect on hatching time. When compared to normoxia, the hatching under severe hypoxia occurred sooner under cooler temperatures (20-50 hours earlier) and was delayed under warming (30-50 hours later; Fig. 4, Fig. S9). This suggests that at warm temperatures and hypoxia, oxygen can become limiting to metabolic processes, leading to slowed development and delayed hatching. At low temperatures, however, where metabolic demands are reduced, the low oxygen saturation in hypoxia may be sufficient to sustain development, but can still induce premature hatching. Together, these results demonstrate a complex interaction between temperature and oxygen availability, whereby severe hypoxia accelerates hatching under cooler temperatures but delays hatching under warming.

Thermal performance curves reveal a broad thermal window for embryonic development

The thermal window for successful zebrafish embryonic development and hatching (>80% success) ranged from 20 to 36 °C under normoxia. This is a broader thermal window than what has previously been reported for zebrafish (~22-34 °C) (Schirone and Gross, 1968; Schnurr et al., 2014; Urushibata et al., 2021). A possible explanation for this discrepancy is that the current experiment used the JU strain of wild-caught zebrafish that have previously been found to be more plastic than the domesticated AB strain (Morgan et al., 2022; Sundin et al., 2019). The thermal range is also narrower, especially on the cold side, than the established thermal window found for juveniles and adults under chronic conditions (Åsheim et al., 2020; Morgan et al., 2019, 2022). A sharp decline in hatching success and complete failure below 18 °C and above 36 °C under all water oxygen levels marks clear thermal limits for the zebrafish embryogenesis. Thermal performance curves further revealed that intermediate temperatures (25-34 °C) maximized yolk sac consumption and larval size, suggesting that this range may support the most efficient energy allocation to growth. Taken together, the embryonic development of zebrafish has a broad thermal window and is surprisingly robust to thermal challenges.

Developmental heat and severe hypoxia marginally shape juvenile thermal limits

Developmental plasticity, whereby early life conditions confer lasting effects across subsequent life stages, has been suggested to be an important mechanism shaping ectotherm thermal tolerance (Scott and Johnston, 2012; Noble et al., 2018). Acute thermal tolerance tests of juveniles showed that early-life exposure to severe hypoxia and non-optimal temperatures can have lasting, albeit modest, effects. Fish reared under severe hypoxia exhibited slightly lower CT_{max} than those reared under normoxia (0.3-0.4 °C average difference; Fig. 7). Similarly, fish reared at colder or warmer temperature extremes showed reduced thermal tolerance relative to those reared near the thermal optimum (0.3 and 0.4 °C average difference, respectively). These effects should be interpreted cautiously, as severe hypoxia and warming caused substantial mortality during early development, such that CT_{max} estimates reflect only individuals that survived to the juvenile stage and do not capture responses across the full range of developmental conditions. Notably, higher developmental temperatures did not enhance juvenile heat tolerance, indicating limited capacity for beneficial developmental plasticity under warming. Overall, the effect sizes associated with developmental plasticity were small, consistent with meta-analyses showing that ectotherm thermal tolerance is only weakly influenced by developmental temperature (Pottier et al., 2022). Together, these results suggest that while early-life oxygen and thermal stress can influence later thermal limits, their effects are modest and do not confer increased tolerance to acute warming.

Conclusion

Early life stages have been viewed as a thermal bottleneck in the fish life cycle, with warming expected to constrain performance through oxygen limitation. Our results challenge the view that oxygen limitation sets the upper thermal boundary for early fish development. Hyperoxia failed to improve early-life performance at high temperatures, and at the upper thermal extremes even reduced hatching success, suggesting potential physiological costs of elevated oxygen under heat stress. Although such costs (e.g. ROS production or oxygen toxicity; Birnie-Gauvin et al., 2016; Tunç et al., 2025) were not directly assessed, the reduced performance under combined warming and hyperoxia could be indicative of such effects. Overall, responses to hyperoxia appear species- and context-dependent.

In contrast, zebrafish embryos tolerated moderate hypoxia remarkably well, and only severe hypoxia combined with warming impaired development and reduced larval survival. While signs of oxygen limitation emerged under these extreme conditions, developmental failure at high temperatures was not alleviated by additional oxygen. This indicates that mechanisms other than oxygen supply, likely involving cellular and molecular limits, constrain the upper thermal tolerance in early life. The broad temperature range supporting successful hatching further highlights the plasticity of embryonic development in zebrafish. Our study also indicates only limited carry over effects of early developmental conditions on later thermal tolerance. Together, these findings underscore the need to understand how multiple interacting stressors affect early developmental stages to more accurately predict species resilience and vulnerability in a warming world.

Acknowledgements

We thank Eline Østduun for their help with fish husbandry and Claudia Hernández Camacho for her assistance during the data collection for the first experiment. Thanks to Nicole Aberle-Malzahn for designing and the NTNU workshop with Øystein Gjervan Hagemo and Robert Karlsen for constructing the thermal gradient table.

Funding sources

This work was supported by the Research Council of Norway (funding scheme for independent projects [FRIPRO] grant FJ: 262942), European Research Council [ERC] (consolidator grant FJ: CLIMEVOLVE), Marie Skłodowska-Curie Actions Grant (grant RE: 893895), and NTNU PhD grant (grant LSG: 976000112).

CRediT authorship contribution statement

Lorena Silva-Garay: Conceptualization, Methodology, Investigation, Data collection, Writing – original draft, Data curation, Visualization, Formal analysis, Project administration. **Moa Metz:** Conceptualization, Methodology, Data collection, Review & Editing. **Henning H. Kristiansen:** Methodology, Data collection, Data curation, Visualization, Review & Editing. **Leon Pfeufer:** Methodology, Data collection, Review & Editing. **Emily Lechner:** Methodology, Data collection, Review & Editing. **Rasmus Ern:** Conceptualization, Methodology, Review & Editing. **Anna H. Andreassen:** Conceptualization, Methodology,

Review & Editing. **Fredrik Jutfelt:** Conceptualization, Methodology, Investigation, Writing – Review & Editing, Validation, Supervision, Resources, Funding acquisition.

References

Abràmoff, M. D., Magalhães, P. J., & Ram, S. J. (2004). Image processing with ImageJ. *Biophotonics international*, *11*(7), 36-42.

Alderdice, D. F., Wickett, W. P., & Brett, J. R. (1958). Some effects of temporary exposure to low dissolved oxygen levels on pacific salmon eggs. *Journal of the Fisheries Research Board of Canada*, *15*(2), 229-250. https://doi.org/10.1139/f58-013

Andreassen, A. H., Hall, P., Khatibzadeh, P., Jutfelt, F., & Kermen, F. (2022). Brain dysfunction during warming is linked to oxygen limitation in larval zebrafish. *Proceedings of the National Academy of Sciences*, *119*(39), e2207052119. https://doi.org/doi:10.1073/pnas.2207052119

Åsheim, E. R., Andreassen, A. H., Morgan, R., & Jutfelt, F. (2020). Rapid-warming tolerance correlates with tolerance to slow warming but not growth at non-optimal temperatures in zebrafish. *Journal of Experimental Biology*, *223*(23). https://doi.org/10.1242/jeb.229195

Barrionuevo, W. R., & Burggren, W. W. (1999). O_2 consumption and heart rate in developing zebrafish (*Danio rerio*): influence of temperature and ambient O_2. *American Journal of Physiology-Regulatory, Integrative and Comparative Physiology*, *276*(2), R505-R513. https://doi.org/10.1152/ajpregu.1999.276.2.R505

Birnie-Gauvin, K., Costantini, D., Cooke, S. J., & Willmore, W. G. (2017). A comparative and evolutionary approach to oxidative stress in fish: A review. *Fish and Fisheries*, *18*(5), 928-942. https://doi.org/https://doi.org/10.1111/faf.12215

Burnham, K. P., & Anderson, D. R. (2004). Multimodel inference: understanding AIC and BIC in model selection. *Sociological Methods & Research*, *33*(2), 261-304. https://doi.org/10.1177/0049124104268644

Burt, P., & Adelson, E. (1983). The Laplacian Pyramid as a compact image code. *IEEE Transactions on Communications*, *31*(4), 532-540. https://doi.org/10.1109/TCOM.1983.1095851

Ciuhandu, C. S., Stevens, E. D., & Wright, P. A. (2005). The effect of oxygen on the growth of *Oncorhynchus mykiss* embryos with and without a chorion. *Journal of Fish Biology*, *67*(6), 1544-1551. https://doi.org/https://doi.org/10.1111/j.1095-8649.2005.00856.x

Comte, L., & Olden, J. D. (2017). Climatic vulnerability of the world's freshwater and marine fishes. *Nature Climate Change*, *7*(10), 718-722. https://doi.org/10.1038/nclimate3382

Cowan, Z.-L., Andreassen, A. H., De Bonville, J., Green, L., Binning, S. A., Silva-Garay, L., Jutfelt, F., & Sundin, J. (2023). A novel method for measuring acute thermal tolerance in fish embryos. *Conservation Physiology*, *11*(1). https://doi.org/10.1093/conphys/coad061

Cowan, Z.-L., Green, L., Clark, T. D., Blewett, T. A., De Bonville, J., Gagnon, T., Hoots, E., Kuchenmüller, L., Leeuwis, R. H. J., Navajas Acedo, J., Rowsey, L. E., Scheuffele, H., Skeeles, M. R., Silva-Garay, L., Jutfelt, F., & Binning, S. A. (2024). Global

change and premature hatching of aquatic embryos. *Global Change Biology*, *30*(9), e17488. https://doi.org/https://doi.org/10.1111/gcb.17488

Czerkies, P., Brzuzan, P., Kordalski, K., & Luczynski, M. (2001). Critical partial pressures of oxygen causing precocious hatching in *Coregonus lavaretus* and *C. albula* embryos. *Aquaculture*, *196*(1), 151-158. https://doi.org/https://doi.org/10.1016/S0044-8486(00)00545-7

Czerkies, P., Kordalski, K., Golas, T., Krysinski, D., & Luczynski, M. (2002). Oxygen requirements of whitefish and vendace (Coregoninae) embryos at final stages of their development. *Aquaculture*, *211*(1), 375-385. https://doi.org/https://doi.org/10.1016/S0044-8486(02)00049-2

Dahlke, F. T., Wohlrab, S., Butzin, M., & Pörtner, H.-O. (2020). Thermal bottlenecks in the life cycle define climate vulnerability of fish. *Science*, *369*(6499), 65-70. https://doi.org/doi:10.1126/science.aaz3658

De Silva, C. (1974). Development of the respiratory system in herring and plaice larvae. In J. H. S. Blaxter, *The Early Life History of Fish* Berlin, Heidelberg.

Dimichele, L., & Taylor, M. H. (1980). The environmental control of hatching in *Fundulus heteroclitus*. *Journal of Experimental Zoology*, *214*(2), 181-187. https://doi.org/https://doi.org/10.1002/jez.1402140209

Du, W.-G., & Shine, R. (2022). The behavioural and physiological ecology of embryos: responding to the challenges of life inside an egg. *Biological Reviews*, *97*(4), 1272-1286. https://doi.org/https://doi.org/10.1111/brv.12841

Ern, R., Johansen, J. L., Rummer, J. L., & Esbaugh, A. J. (2017). Effects of hypoxia and ocean acidification on the upper thermal niche boundaries of coral reef fishes. *Biology Letters*, *13*(7), 20170135. https://doi.org/doi:10.1098/rsbl.2017.0135

Ern, R., Norin, T., Gamperl, A. K., & Esbaugh, A. J. (2016). Oxygen dependence of upper thermal limits in fishes. *Journal of Experimental Biology*, *219*(21), 3376-3383. https://doi.org/10.1242/jeb.143495

Fry, F. E. J., & Hart, J. S. (1948). The relation of temperature to oxygen consumption in the goldfish. *The Biological Bulletin*, *94*(1), 66-77. https://doi.org/10.2307/1538211

Garside, E. T. (1966). Effects of oxygen in relation to temperature on the development of embryos of Brook trout and Rainbow trout. *Journal of the Fisheries Research Board of Canada*, *23*(8), 1121-1134. https://doi.org/10.1139/f66-105

Gierten, J., Pylatiuk, C., Hammouda, O. T., Schock, C., Stegmaier, J., Wittbrodt, J., Gehrig, J., & Loosli, F. (2020). Automated high-throughput heartbeat quantification in medaka and zebrafish embryos under physiological conditions. *Scientific Reports*, *10*(1), 2046. https://doi.org/10.1038/s41598-020-58563-w

Hassell, K. L., Coutin, P. C., & Nugegoda, D. (2008). Hypoxia impairs embryo development and survival in black bream (*Acanthopagrus butcheri*). *Marine Pollution Bulletin*, *57*(6), 302-306. https://doi.org/https://doi.org/10.1016/j.marpolbul.2008.02.045

Haugen, L. A. S. (2022). *Feeding ecology and behavior of nudibranchs from the sublittoral zones of Trondheimsfjorden and interactions with fouling communities* [Master's thesis Norwegian University of Science and Technology].

Hayes, F. R., Wilmot, I. B., & Livingstone, D. A. (1951). The oxygen consumption of the salmon egg in relation to development and activity. *Journal of Experimental Zoology*, *116*(3), 377-395. https://doi.org/https://doi.org/10.1002/jez.1401160302

Jonz, M. G., & Nurse, C. A. (2005). Development of oxygen sensing in the gills of zebrafish. *Journal of Experimental Biology*, *208*(8), 1537-1549. https://doi.org/10.1242/jeb.01564

Kamiński, R., Kamler, E., Korwin-Kossakowski, M., Myszkowski, L., & Wolnicki, J. (2006). Effects of different incubation temperatures on the yolk-feeding stage of *Eupallasella*

percnurus (Pallas). *Journal of Fish Biology*, *68*(4), 1077-1090. https://doi.org/https://doi.org/10.1111/j.0022-1112.2006.01008.x

Kamler, E., Szlamińska, M., Kuczyński, M., Hamáčková, J., Kouřil, J., & Dabrowski, R. (1994). Temperature-induced changes of early development and yolk utilization in the African catfish *Clarias gariepinus*. *Journal of Fish Biology*, *44*(2), 311-326. https://doi.org/https://doi.org/10.1111/j.1095-8649.1994.tb01208.x

Keckeis, H., Bauer-Nemeschkal, E., & Kamler, E. (1996). Effects of reduced oxygen level on the mortality and hatching rate of *Chondrostoma nasus* embryos. *Journal of Fish Biology*, *49*(3), 430-440. https://doi.org/https://doi.org/10.1111/j.1095-8649.1996.tb00039.x

Kimmel, C. B., Ballard, W. W., Kimmel, S. R., Ullmann, B., & Schilling, T. F. (1995). Stages of embryonic development of the zebrafish. *Developmental Dynamics*, *203*(3), 253-310. https://doi.org/https://doi.org/10.1002/aja.1002030302

Latham, K. E., & Just, J. J. (1989). Oxygen availability provides a signal for hatching in the rainbow trout (*Salmo gairdneri*) embryo. *Canadian Journal of Fisheries and Aquatic Sciences*, *46*(1), 55-58. https://doi.org/10.1139/f89-008

Lauridsen, H., Gonzales, S., Hedwig, D., Perrin, K. L., Williams, C. J. A., Wrege, P. H., Bertelsen, M. F., Pedersen, M., & Butcher, J. T. (2019). Extracting physiological information in experimental biology via Eulerian video magnification. *BMC Biology*, *17*(1), 103. https://doi.org/10.1186/s12915-019-0716-7

Marks, C., Kaut, K. P., Moore, F. B.-G., & Bagatto, B. (2012). Ontogenetic oxygen changes alter zebra fish size, behavior, and blood glucose. *Physiological and Biochemical Zoology*, *85*(6), 635-644. https://doi.org/10.1086/666508

McArley, T. J., Morgenroth, D., Zena, L. A., Ekström, A. T., & Sandblom, E. (2022). Prevalence and mechanisms of environmental hyperoxia-induced thermal tolerance in fishes. *Proceedings of the Royal Society B: Biological Sciences*, *289*(1981), 20220840. https://doi.org/doi:10.1098/rspb.2022.0840

Miller, S. C., Reeb, S. E., Wright, P. A., & Gillis, T. E. (2008). Oxygen concentration in the water boundary layer next to rainbow trout (*Oncorhynchus mykiss*) embryos is influenced by hypoxia exposure time, metabolic rate, and water flow. *Canadian Journal of Fisheries and Aquatic Sciences*, *65*(10), 2170-2177. https://doi.org/10.1139/f08-123

Morgan, R., Andreassen, A. H., Åsheim, E. R., Finnøen, M. H., Dresler, G., Brembu, T., Loh, A., Miest, J. J., & Jutfelt, F. (2022). Reduced physiological plasticity in a fish adapted to stable temperatures. *Proceedings of the National Academy of Sciences*, *119*(22), e2201919119. https://doi.org/doi:10.1073/pnas.2201919119

Morgan, R., Finnøen, M. H., & Jutfelt, F. (2018). CTmax is repeatable and doesn't reduce growth in zebrafish. *Scientific Reports*, *8*(1), 7099. https://doi.org/10.1038/s41598-018-25593-4

Morgan, R., Sundin, J., Finnøen, M. H., Dresler, G., Vendrell, M. M., Dey, A., Sarkar, K., & Jutfelt, F. (2019). Are model organisms representative for climate change research? Testing thermal tolerance in wild and laboratory zebrafish populations. *Conservation Physiology*, *7*(1). https://doi.org/10.1093/conphys/coz036

Mueller, C. A., Joss, J. M. P., & Seymour, R. S. (2011). Effects of environmental oxygen on development and respiration of Australian lungfish (*Neoceratodus forsteri*) embryos. *Journal of Comparative Physiology B*, *181*(7), 941-952. https://doi.org/10.1007/s00360-011-0573-3

Myrvold, S. L. (2020). *Effect of temperature on the settling rate, survival, ingestion rate and biochemical composition of the polyp stages of A. aurita* [Master's thesis, Norwegian University of Science and Technology].

Negrete, B., Jr, Ackerly, K. L., & Esbaugh, A. J. (2024). Implications of chronic hypoxia during development in red drum. *Journal of Experimental Biology*, *227*(16). https://doi.org/10.1242/jeb.247618

Noble, D. W. A., Stenhouse, V., & Schwanz, L. E. (2018). Developmental temperatures and phenotypic plasticity in reptiles: a systematic review and meta-analysis. *Biological Reviews*, *93*(1), 72-97. https://doi.org/https://doi.org/10.1111/brv.12333

Pörtner, H.-O. (2010). Oxygen- and capacity-limitation of thermal tolerance: a matrix for integrating climate-related stressor effects in marine ecosystems. *Journal of Experimental Biology*, *213*(6), 881-893. https://doi.org/10.1242/jeb.037523

Pörtner, H.-O., Bock, C., & Mark, F. C. (2017). Oxygen- and capacity-limited thermal tolerance: bridging ecology and physiology. *Journal of Experimental Biology*, *220*(15), 2685-2696. https://doi.org/10.1242/jeb.134585

Pottier, P., Burke, S., Drobniak, S. M., & Nakagawa, S. (2022). Methodological inconsistencies define thermal bottlenecks in fish life cycle: a comment on Dahlke et al. 2020. *Evolutionary Ecology*, *36*(2), 287-292. https://doi.org/10.1007/s10682-022-10157-w

Raby, G. D., De Bonville, J., Reynolds, L., Storm, Z., Cowan, Z.-L., Metz, M., Andreassen, A. H., Pfeufer, L., Lechner, E. R., Stewart, E. M. C., Leeuwis, R. H. J., Ern, R., Silva-Garay, L., Skeeles, M. R., Roche, D. G., Morgan, R., Green, L., Speers-Roesch, B., Mills, S. C., . . . Jutfelt, F. (2025). Oxygen supersaturation has negligible effects on warming tolerance across diverse aquatic ectotherms. *PLOS Biology*, *23*(11), e3003413. https://doi.org/10.1371/journal.pbio.3003413

Rombough, P. J. (1989). Oxygen conductance values and structural characteristics of the egg capsules of pacific salmonids. *Comparative Biochemistry and Physiology Part A: Physiology*, *92*(3), 279-283. https://doi.org/https://doi.org/10.1016/0300-9629(89)90564-1

Rombough, P. J. (1999). The gill of fish larvae. Is it primarily a respiratory or an ionoregulatory structure? *Journal of Fish Biology*, *55*(sA), 186-204. https://doi.org/https://doi.org/10.1111/j.1095-8649.1999.tb01055.x

Schirone, R. C., & Gross, L. (1968). Effect of temperature on early embryological development of the zebra fish, *Brachydanio rerio*. *Journal of Experimental Zoology*, *169*(1), 43-52. https://doi.org/https://doi.org/10.1002/jez.1401690106

Schnurr, M. E., Yin, Y., & Scott, G. R. (2014). Temperature during embryonic development has persistent effects on metabolic enzymes in the muscle of zebrafish. *Journal of Experimental Biology*, *217*(8), 1370-1380. https://doi.org/10.1242/jeb.094037

Scott, G. R., & Johnston, I. A. (2012). Temperature during embryonic development has persistent effects on thermal acclimation capacity in zebrafish. *Proceedings of the National Academy of Sciences*, *109*(35), 14247-14252. https://doi.org/10.1073/pnas.1205012109

Shumway, D. L., Warren, C. E., & Doudoroff, P. (1964). Influence of oxygen concentration and water movement on the growth of steelhead trout and coho salmon embryos. *Transactions of the American Fisheries Society*, *93*(4), 342-356. https://doi.org/10.1577/1548-8659(1964)93[342:Ioocaw]2.0.Co;2

Silva-Garay, L., Ern, R., Andreassen, A. H., Reiersen, M., & Jutfelt, F. (2025). No oxygen limitation of upper thermal tolerance in zebrafish regardless of acclimation temperature. *Journal of Thermal Biology*, *131*, 104157. https://doi.org/https://doi.org/10.1016/j.jtherbio.2025.104157

Skeeles, M. R., Scheuffele, H., & Clark, T. D. (2022). Chronic experimental hyperoxia elevates aerobic scope: a valid method to test for physiological oxygen limitations in

fish. *Journal of Fish Biology*, *101*(6), 1595-1600. https://doi.org/https://doi.org/10.1111/jfb.15213

Sunday, J. M., Bates, A. E., & Dulvy, N. K. (2012). Thermal tolerance and the global redistribution of animals. *Nature Climate Change*, *2*(9), 686-690. https://doi.org/10.1038/nclimate1539

Sundin, J., Morgan, R., Finnøen, M. H., Dey, A., Sarkar, K., & Jutfelt, F. (2019). On the observation of wild zebrafish (*Danio rerio*) in India. *Zebrafish*, *16*(6), 546-553. https://doi.org/10.1089/zeb.2019.1778

Teletchea, F., & Pauly, D. (2024). Why do fish larvae hatch when they do? *Environmental Biology of Fishes*, *107*(5), 583-591. https://doi.org/10.1007/s10641-024-01553-y

Thomas, W. H., Scotten, H. L., & Bradshaw, J. S. (1963). Thermal gradient incubators for small aquatic organisms *Limnology and Oceanography*, *8*(3), 357-360. https://doi.org/https://doi.org/10.4319/lo.1963.8.3.0357

Tunç, A., Erdoğan, O., Vural, O., & Aksakal, E. (2025). Impact of acute and long-term hypoxia and hyperoxia on antioxidant metabolism and gene expression in juvenile rainbow trout (*Oncorhynchus mykiss*). *Aquaculture Research*, *2025*(1), 6628284. https://doi.org/https://doi.org/10.1155/are/6628284

Urushibata, H., Sasaki, K., Takahashi, E., Hanada, T., Fujimoto, T., Arai, K., & Yamaha, E. (2021). Control of developmental speed in zebrafish embryos using different incubation temperatures. *Zebrafish*, *18*(5), 316-325. https://doi.org/10.1089/zeb.2021.0022

Warkentin, K. M. (2007). Oxygen, gills, and embryo behavior: mechanisms of adaptive plasticity in hatching. *Comparative Biochemistry and Physiology Part A: Molecular & Integrative Physiology*, *148*(4), 720-731. https://doi.org/https://doi.org/10.1016/j.cbpa.2007.02.009

Warkentin, K. M. (2011). Environmentally cued hatching across taxa: embryos respond to risk and opportunity. *Integrative and Comparative Biology*, *51*(1), 14-25. https://doi.org/10.1093/icb/icr017

Wells, P. R., & Pinder, A. W. (1996). The respiratory development of atlantic salmon: I. morphometry of gills, yolk sac and body surface. *Journal of Experimental Biology*, *199*(12), 2725-2736. https://doi.org/10.1242/jeb.199.12.2725

Wood, A. T., Clark, T. D., Elliott, N. G., Frappell, P. B., & Andrewartha, S. J. (2019). Physiological effects of dissolved oxygen are stage-specific in incubating Atlantic salmon (*Salmo salar*). *Journal of Comparative Physiology B*, *189*(1), 109-120. https://doi.org/10.1007/s00360-018-1199-5

Supplementary Information for

Oxygen limitation is not a major physiological mechanism restricting early life development in zebrafish

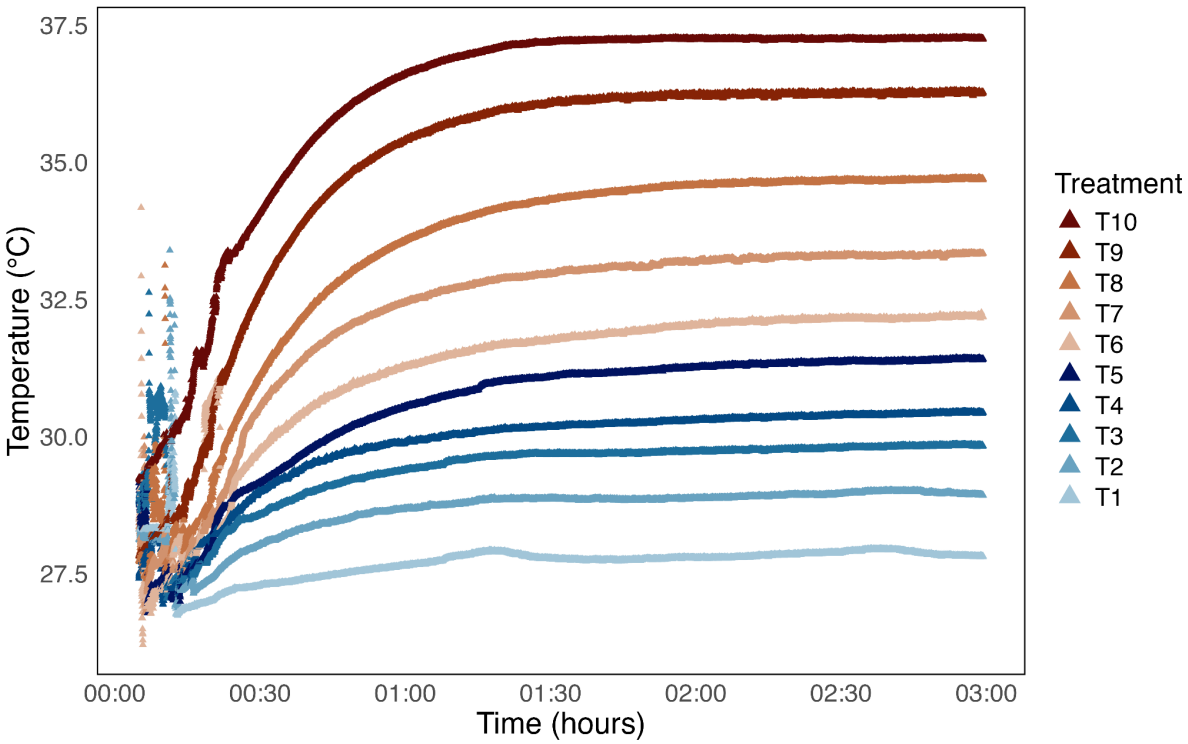

Fig. S1: Heating rate across treatments in the thermal gradient table.
Heating rate (°C h^{-1}) over time in beakers used in *Experiment 2*. Treatments differ by color and correspond to distinct temperature change profiles established in the thermal gradient table.

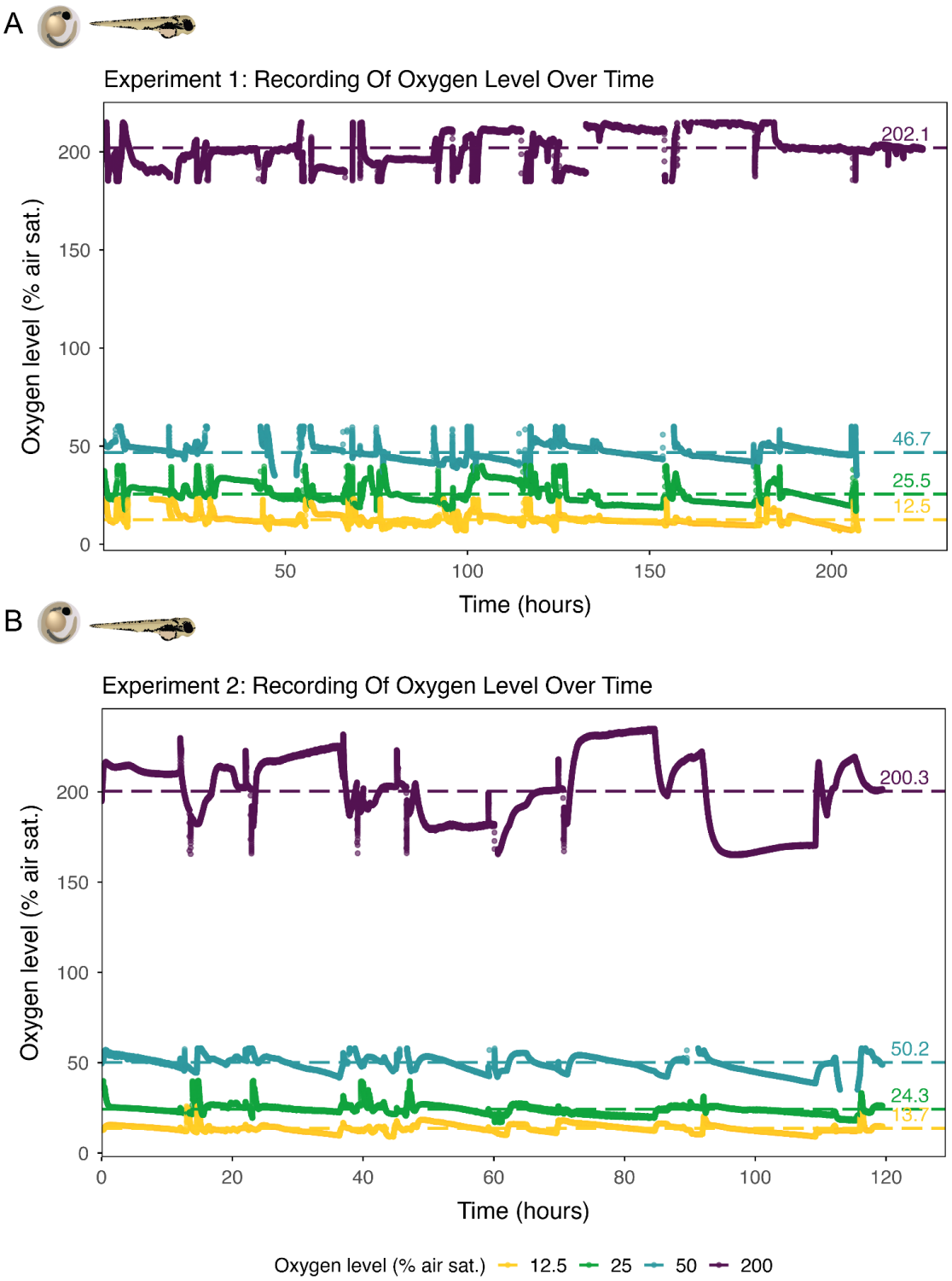

Fig. S2: Oxygen records over the total experimental time (in hours) of *Experiment 1* and *Experiment 2*. Raw data and means of the target oxygen treatments during experiments are depicted in colors. *Experiment 1* lasted ~ 10 days and *Experiment 2* lasted ~ 6 days.

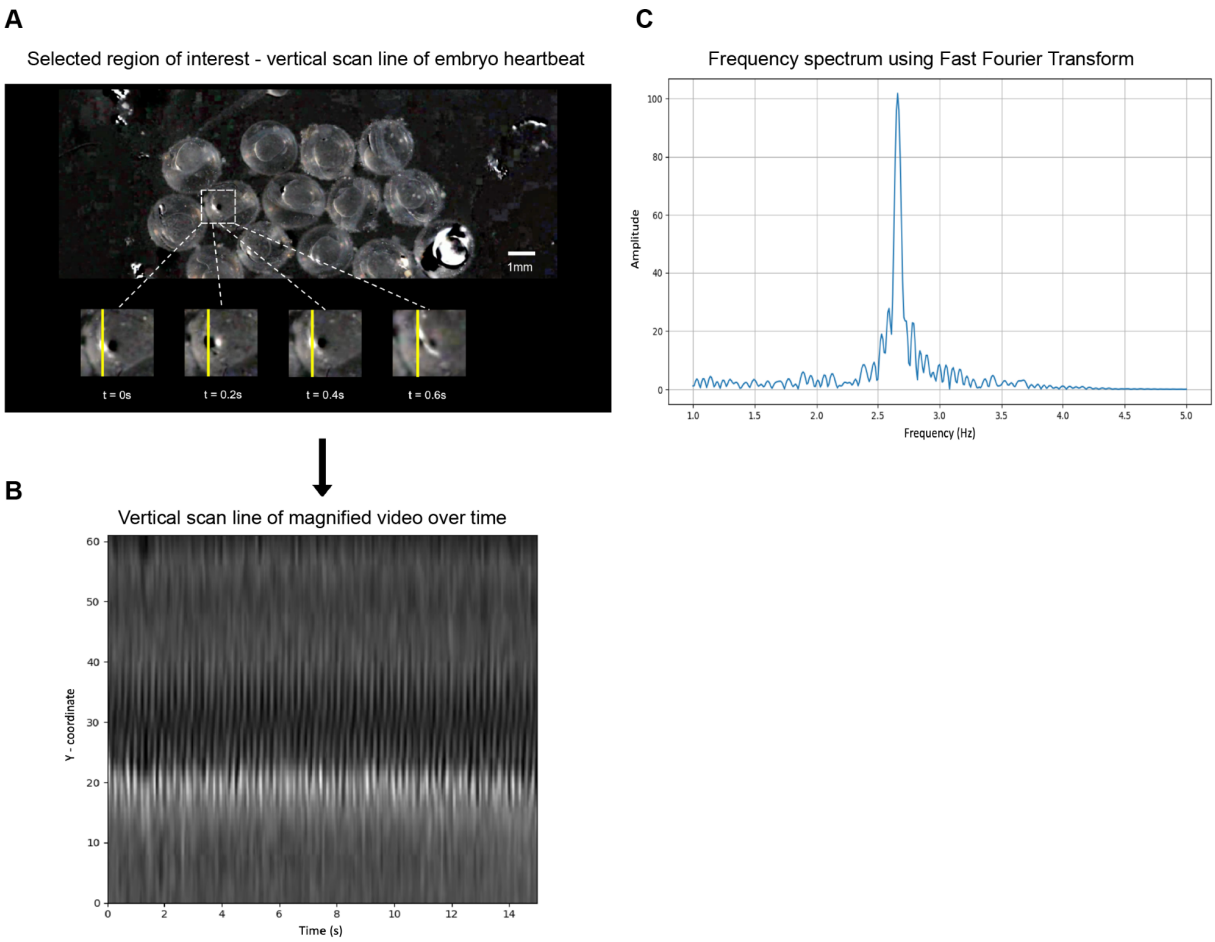

Fig. S3: Measurement of heart rate in zebrafish embryos using Eulerian video magnification. (A) Cropped video frame showing the embryonic heart of *Danio rerio*. The yellow vertical line marks the region where the heartbeat is most visible across the recording, with periodic pixel contrast shifts (white to black) reflecting heartbeat frequency. **(B)** Time-series plot of pixel contrast variation along the yellow line over a 15 s recording, capturing rhythmic heartbeat oscillations. **(C)** Frequency spectrum derived from the same region using a Fast Fourier Transform, showing the dominant heartbeat frequency (Hz). A sharp amplitude peak indicates a strong signal with low noise and a stable heart rate.

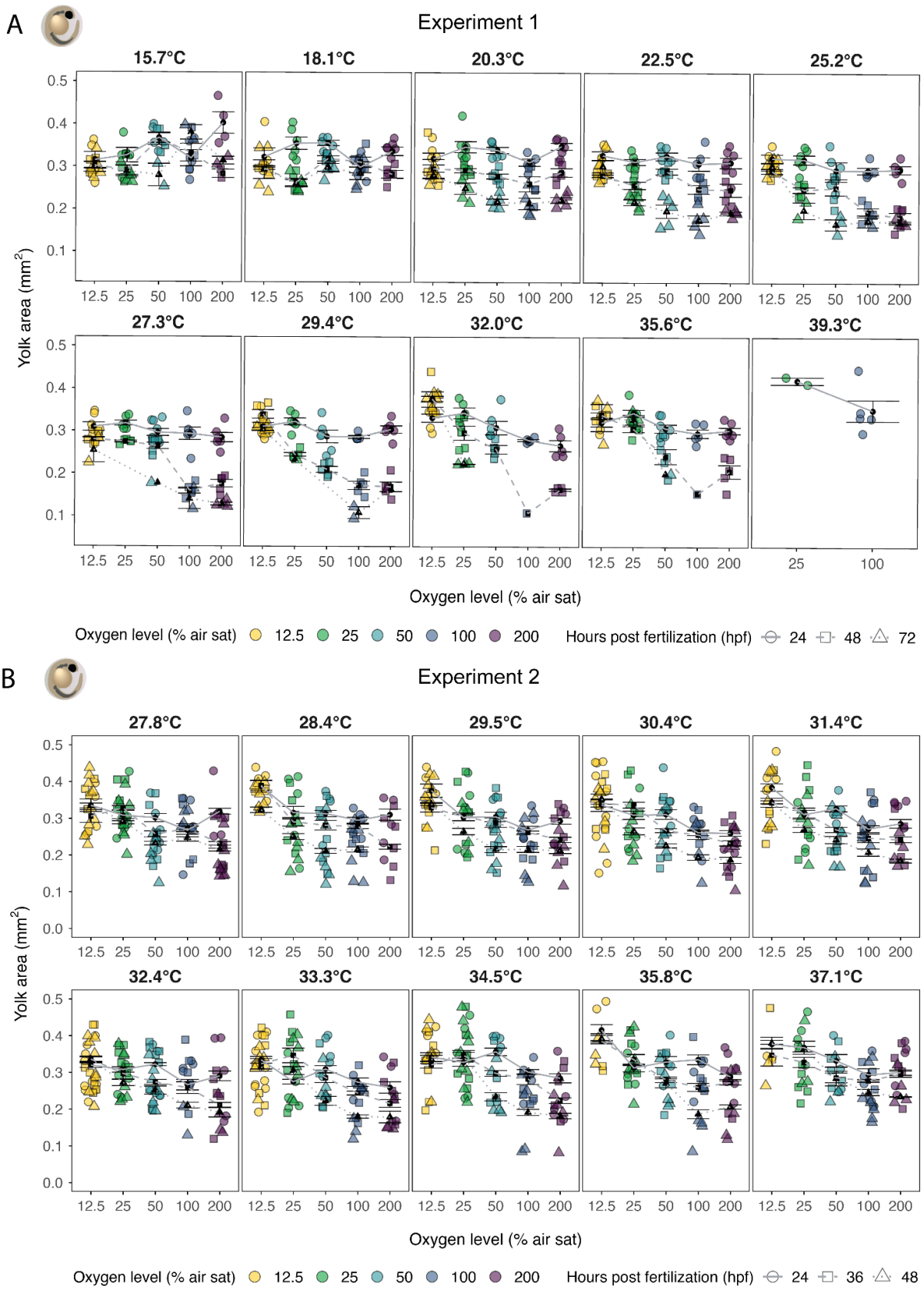

Fig. S4: Yolk sac area of zebrafish embryos across temperature, oxygen, and developmental time. Yolk sac area (mm²) of *Danio rerio* embryos across oxygen levels (colors) and temperatures (vertical panels) over time post-fertilization. Measurements were

taken at 24, 48, and 72 hpf in *Experiment 1*, and at 24, 36, and 48 hpf in *Experiment 2*. Data points represent individual embryos; black triangles indicate group means ± s.e., and grey dashed lines connect mean values across sampling times.

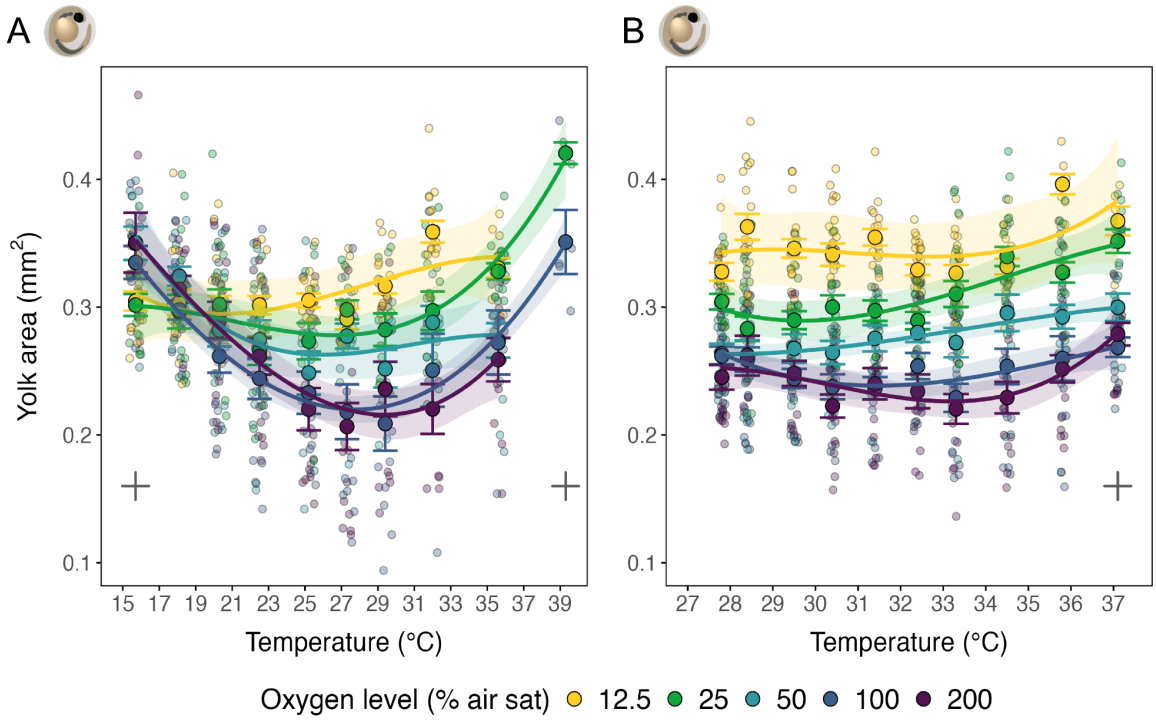

Fig. S5: Yolk sac area (mm²) of zebrafish embryos across temperatures (x-axis) and oxygen levels (colors) in *Experiment 1* (A; n = 2–9) **and *Experiment 2*** (B; n = 2–11). Points show individual embryos; colored circles indicate means ± s.e., and colored lines indicating second-degree polynomial fits.

Table S1: Yolk sac consumption (%) of zebrafish embryos across temperature, oxygen, and developmental time in *Experiment 1*. Anova (type III) and linear model (LM) includes oxygen level, temperature centered to 15.7 °C ($Temp_1$), and its quadratic term ($Temp_2$), their interaction, and developmental time (hpf): Yolk consumption ~ O_2 + $Temp_1$ + $Temp_2$ + O_2×$Temp_1$ + O_2×$Temp_2$ + hpf. Significance was assessed relative to 15.7 °C and 100% air saturation. Estimates (β), standard errors (SE), t-values, and p-values are shown for each predictor.

Parameters (Anova, type III)	*Sum Squares*	*Df*	*F-value*	*P-value*
(Intercept)	581	1	6.4054	0.0116*
O_2	1688	4	4.6523	0.0011**
$Temp_1$	11172	1	123.1568	< 0.0001 ***
$Temp_2$	8455	1	93.2098	< 0.0001 ***
O_2:$Temp_1$	5232	4	14.4203	< 0.0001 ***
O_2:$Temp_2$	2006	4	5.5294	0.0002***

hpf	37213	1	410.2245	< 0.0001 ***
Residuals	53975	595		

Parameters (LM)	*Estimate (B)*	*Std. Error*	*t-value*	*P-value*
(Intercept)	-5.860	2.315	-2.531	0.012 *
O_2(12.5%)	7.661	2.879	2.661	0.008 **
O_2(25%)	6.136	2.853	2.151	0.032 *
O_2(50%)	-2.182	3.021	-0.722	0.470
O_2(200%)	-1.163	3.292	-0.353	0.724
$Temp_1$	5.014	0.452	11.098	< 0.0001 ***
$Temp_2$	-0.195	0.020	-9.655	< 0.0001 ***
hpf	0.429	0.021	20.254	< 0.0001 ***
O_2(12.5%):$Temp_1$	-4.391	0.648	-6.779	< 0.0001 ***
O_2(25%):$Temp_1$	-2.675	0.635	-4.215	< 0.0001 ***
O_2(50%):$Temp_1$	-1.341	0.678	-1.978	0.048 *
O_2(200%):$Temp_1$	-0.410	0.720	-0.568	0.570
O_2(12.5%):$Temp_2$	0.140	0.031	4.571	< 0.0001 ***
O_2(25%):$Temp_2$	0.073	0.029	2.502	0.013 *
O_2(50%):$Temp_2$	0.064	0.032	2.011	0.045 *
O_2(200%):$Temp_2$	0.035	0.033	1.051	0.294
Residual standard error:	9.524 on 595 degrees of freedom			
Multiple R-squared:	0.6189			
F-statistic:	64.41 on 15 and 595 DF, p-value: < 0.001 ***			

Table S2: Yolk sac consumption (%) of zebrafish embryos across temperature, oxygen, and developmental time in *Experiment 2*. Anova (type III) and linear model (LM) includes oxygen level, temperature centered to 27.8 °C ($Temp_1$), and its quadratic term ($Temp_2$), their interaction, and developmental time (hpf): Yolk consumption ~ O_2 + $Temp_1$ + $Temp_2$ + O_2×$Temp_1$ + O_2×$Temp_2$ + hpf. Significance was assessed relative to 27.8 °C and 100% air saturation. Estimates (β), standard errors (SE), t-values, and p-values are shown for each predictor.

Parameters (Anova, type III)	*Sum Squares*	*Df*	*F-value*	*P-value*
(Intercept)	7128	1	118.067	< 0.0001 ***

O_2	13295	4	55.053	< 0.0001 ***
$Temp_1$	828	1	13.718	0.0002***
$Temp_2$	1046	1	17.325	0.00003***
O_2:$Temp_1$	1288	4	5.334	0.0003***
O_2:$Temp_2$	811	4	3.359	0.0097**
hpf	21395	1	354.368	< 0.0001 ***
Residuals	48482	803		

Parameters (LM)	***Estimate (B)***	***Std. Error***	***t value***	***P-value***
(Intercept)	18.766	1.727	10.866	< 0.0001 ***
O_2(12.5%)	-21.622	1.907	-11.336	< 0.0001 ***
O_2(25%)	-8.598	1.910	-4.503	< 0.0001 ***
O_2(50%)	0.032	1.918	0.016	0.987
O_2(200%)	1.702	1.955	0.871	0.384
$Temp_1$	2.745	0.741	3.704	0.0002 ***
$Temp_2$	-0.325	0.078	-4.162	< 0.0001 ***
hpf	0.520	0.028	18.825	< 0.0001 ***
O_2(12.5%):$Temp_1$	-0.245	1.031	-0.238	0.812
O_2(25%):$Temp_1$	-1.975	1.012	-1.952	0.051
O_2(50%):$Temp_1$	-3.399	1.024	-3.320	0.001 **
O_2(200%):$Temp_1$	0.625	1.042	0.600	0.549
O_2(12.5%):$Temp_2$	0.008	0.116	0.073	0.942
O_2(25%):$Temp_2$	0.087	0.109	0.798	0.425
O_2(50%):$Temp_2$	0.296	0.110	2.687	0.007 **
O_2(200%):$Temp_2$	-0.079	0.111	-0.716	0.474

Residual standard error:	7.77 on 803 degrees of freedom
Multiple R-squared:	0.659
F-statistic:	103.2 on 15 and 803 DF, p-value: < 0.001 ***
Adjusted R-squared:	0.652

Table S3: Heart rate of zebrafish embryos across temperature, oxygen, and developmental time in *Experiment 2*. Anova (type III) and linear model (LM) includes oxygen level, temperature centered to 27.8 °C ($Temp_1$), and its quadratic term ($Temp_2$), their interaction, and developmental time (hpf): Heart rate ~ O_2 + $Temp_1$ + $Temp_2$ + O_2×$Temp_1$ + O_2×$Temp_2$ + hpf. Significance was assessed relative to 27.8 °C and 100% air saturation. Estimates (β), standard errors (SE), t-values, and p-values are shown for each predictor.

Parameters (Anova, type III)	***Sum Squares***	***Df***	***F-value***	***p-value***
(Intercept)	379095	1	219.751	< 0.0001 ***
O_2	338503	4	49.055	< 0.0001 ***
$Temp_1$	47756	1	27.683	< 0.0001 ***
$Temp_2$	48746	1	28.256	< 0.0001 ***
O_2:$Temp_1$	13286	4	1.925	0.1042
O_2:$Temp_2$	11686	4	1.693	0.1494
hpf	748588	1	433.935	< 0.0001 ***
Residuals	1511201	876		
Parameters (LM)	***Estimate (B)***	***Std. Error***	***t-value***	***p-value***
(Intercept)	109.803	7.407	14.824	< 0.0001 ***
O_2(12.5%)	-96.197	8.723	-11.028	< 0.0001 ***
O_2(25%)	-19.152	8.914	-2.149	0.0319*
O_2(50%)	2.098	9.916	0.212	0.8325
O_2(200%)	11.082	9.209	1.203	0.2291
$Temp_1$	19.596	3.724	5.261	< 0.0001 ***
$Temp_2$	-2.193	0.413	-5.316	< 0.0001 ***
hpf	1.628	0.078	20.831	< 0.0001 ***
O_2(12.5%):$Temp_1$	2.775	5.770	0.481	0.6307
O_2(25%):$Temp_1$	-5.969	5.448	-1.096	0.2736
O_2(50%):$Temp_1$	-12.959	5.837	-2.220	0.0267*
O_2(200%):$Temp_1$	-4.209	5.202	-0.809	0.4187
O_2(12.5%):$Temp_2$	-0.301	0.842	-0.357	0.7208
O_2(25%):$Temp_2$	-0.211	0.658	-0.321	0.7481
O_2(50%):$Temp_2$	1.435	0.669	2.144	0.0323*
O_2(200%):$Temp_2$	0.182	0.573	0.318	0.7504

Residual standard error:	41.53 on 876 degrees of freedom
Multiple R-squared:	0.4287
F-statistic:	43.82 on 15 and 876 DF, p-value: < 0.0001 ***
Adjusted R-squared:	0.587

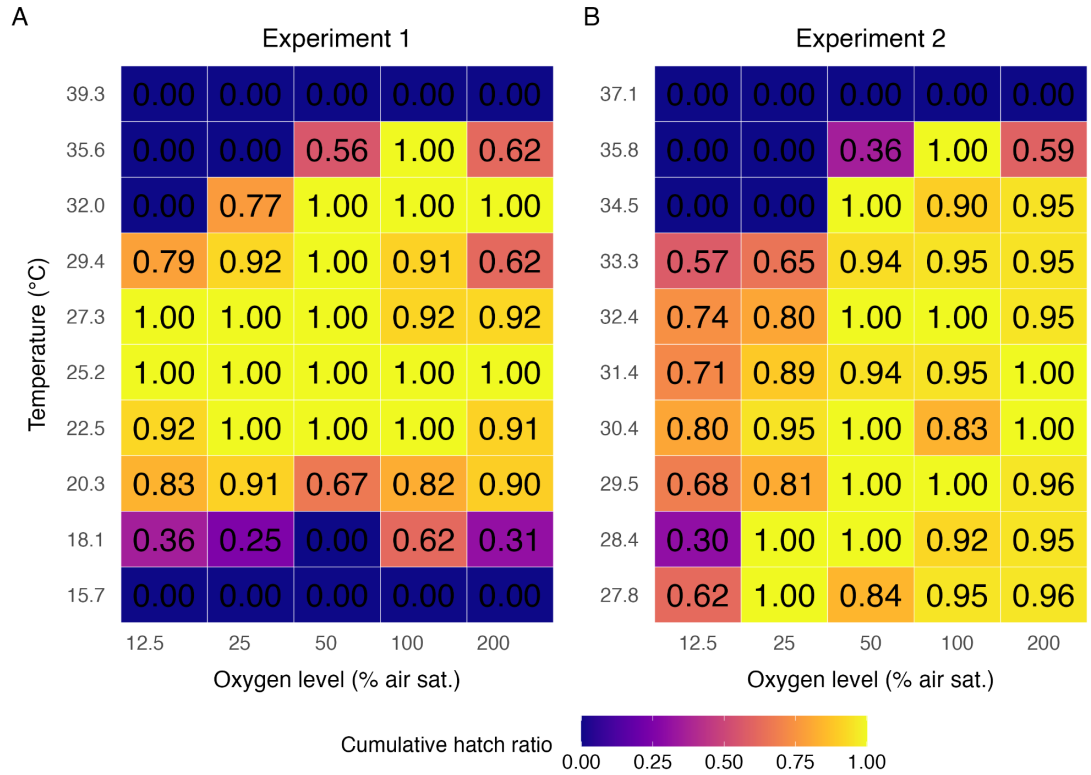

Fig. S6: Heat map of maximum hatching number across temperature and oxygen treatments. Heat map showing the accumulated maximum number of hatched *Danio rerio* embryos per temperature and oxygen treatment in (A) *Experiment 1* and (B) *Experiment 2*. Lighter colors (yellow) indicate higher hatching rates.

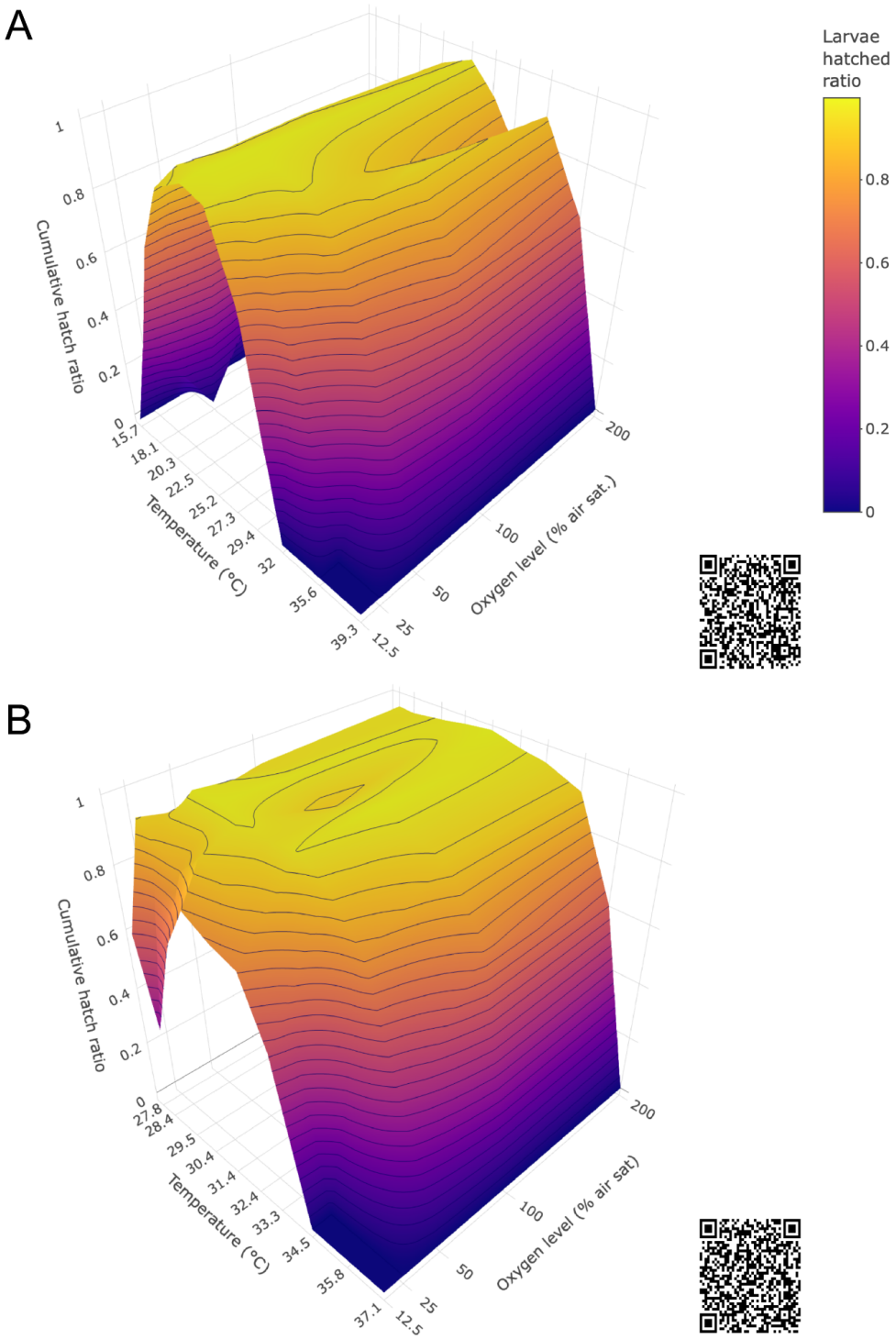

Fig. S7: Three-dimensional surface plot of cumulative hatching across temperature and oxygen treatments. 3D surface plots showing cumulative hatching of *Danio rerio* larvae across temperature and oxygen levels in (A) *Experiment 1* and (B) *Experiment 2*. Cumulative hatching values are based on observed data. Survival ratios above 0.6 were smoothed using a kernel-based normalization. (function image.smoother, aRange = 0.75, theta = 0.75, fields package, R), preventing overfitting when hatching nears zero at the extreme temperatures.

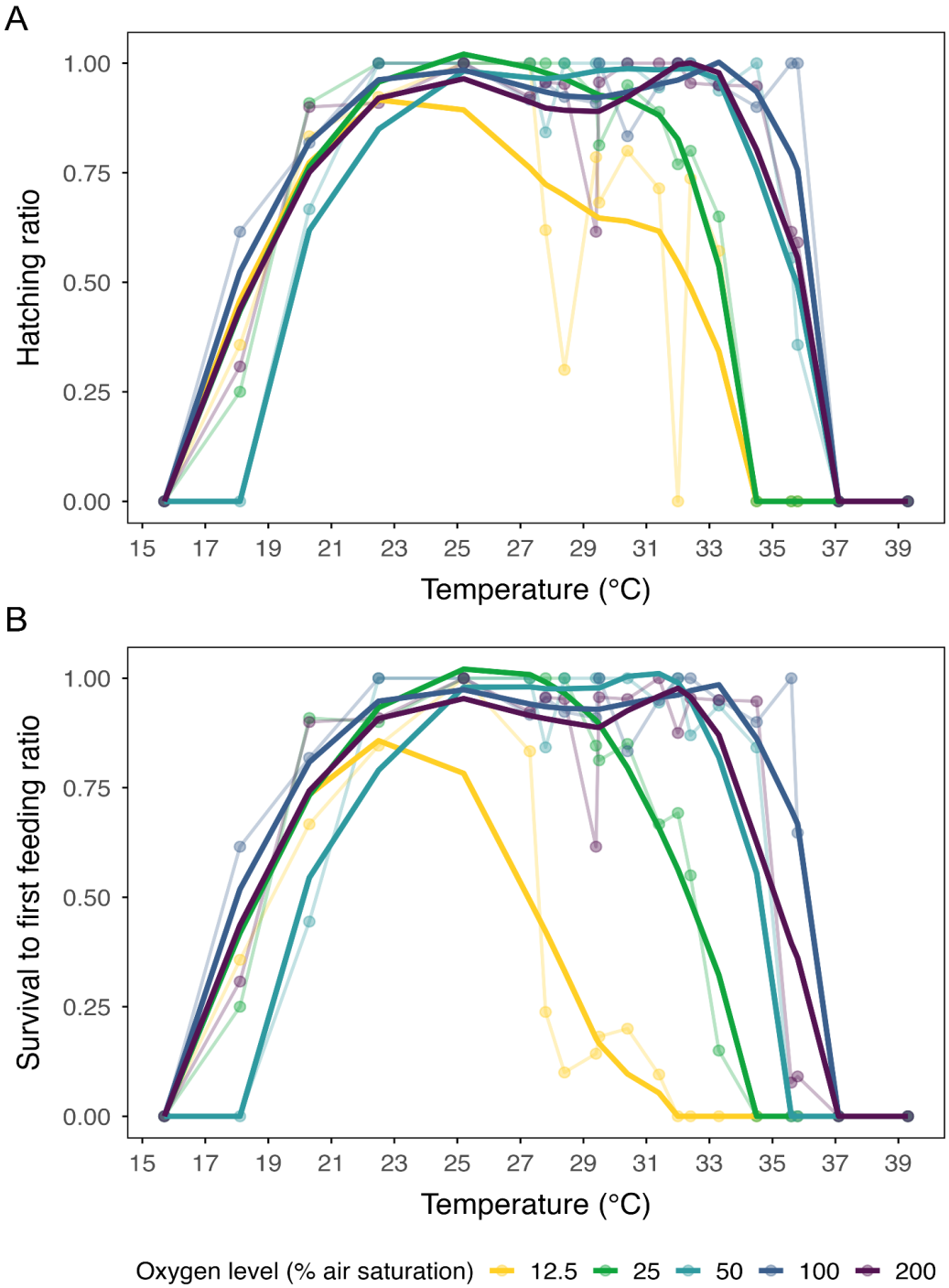

Fig. S8: Thermal performance curve (TPC) of hatching success (A) and survival to first feeding (B) across temperature and oxygen levels. Points depict maximum hatching ratio per temperature, and TPC lines were fitted using a smoothed maxima *LOESS* function (span = 0.6).

Table S4: Effect of oxygen, temperature, and developmental time on hatching success in *Experiment 1*. GLM includes oxygen level, temperature centered to 18.1 °C ($Temp_1$, lowest temperature at which hatching occurred), and its quadratic term ($Temp_2$), their interaction, and log-transformed developmental time (hpf): Hatching success ~ O_2 + $Temp_1$ + $Temp_2$ + O_2×$Temp_1$ + O_2×$Temp_2$ + log(hpf) + (1 | Experiment). Significance is shown first with

oxygen as numeric relative to 18.1 °C and subsequently relative to 100% air saturation. Estimates (β), standard errors (SE), z-values, and p-values are shown for each predictor.

Parameters (GLM)	***Estimate (B)***	***Std. Error***	***z-value***	***p-value***
(Intercept)	-24.4100	0.6950	-35.128	< 0.0001 ***
O_2	-0.0004	0.0015	-0.288	0.773
$Temp_1$	1.3150	0.0484	27.195	< 0.0001 ***
$Temp_2$	-0.0665	0.0027	-24.564	< 0.0001 ***
O_2:$Temp_1$	-0.0017	0.0004	-4.380	0.00001
O_2:$Temp_2$	0.0002	0.0000	7.263	< 0.0001 ***
log(hpf)	4.3400	0.1289	33.654	< 0.0001 ***
Null deviance:		6068.2 on 563 degrees of freedom		
Residual deviance:		1498.8 on 557 degrees of freedom		
AIC:		1959		
Num.Fisher Scoring iterations:		3		

Parameters (GLM)	***Estimate (B)***	***Std. Error***	***z-value***	***p-value***
(Intercept)	-30.6686	0.9320	-32.905	< 0.0001 ***
O_2(12.5%)	-1.1127	0.3523	-3.159	0.0016 **
O_2(25%)	-1.0823	0.3568	-3.033	0.0024 **
O_2(50%)	-3.1413	0.4516	-6.956	< 0.0001 ***
O_2(200%)	-0.6648	0.3208	-2.072	0.0382 *
$Temp_1$	1.0536	0.0597	17.661	< 0.0001 ***
$Temp_2$	-0.0306	0.0030	-10.160	< 0.0001 ***
O_2(12.5%):$Temp_1$	1.0454	0.1155	9.048	< 0.0001 ***
O_2(25%):$Temp_1$	0.9531	0.1106	8.615	< 0.0001 ***
O_2(50%):$Temp_1$	0.9264	0.1129	8.206	< 0.0001 ***
O_2(200%):$Temp_1$	0.1588	0.0833	1.907	0.0565 ·
O_2(12.5%):$Temp_2$	-0.1072	0.0081	-13.310	< 0.0001 ***
O_2(25%):$Temp_2$	-0.0774	0.0069	-11.194	< 0.0001 ***
O_2(50%):$Temp_2$	-0.0527	0.0059	-9.004	< 0.0001 ***
O_2(200%):$Temp_2$	-0.0187	0.0045	-4.159	0.00003 ***
log(hpf)	5.6246	0.1727	32.560	< 0.0001 ***

Null deviance:	6102.34 on 563 degrees of freedom
Residual deviance:	734.34 on 548 degrees of freedom
AIC:	1212.6
Num.Fisher Scoring iterations:	4

Table S5: Effect of oxygen, temperature, and developmental time on hatching success in *Experiment 1*. Effect of oxygen level, temperature, and time post-fertilization (hpf) on hatching success of *Danio rerio* embryos, derived from GLM: Hatching success ~ O_2 × Temp + log(hpf). Post hoc comparisons were conducted relative to the control treatment (27.3 °C, normoxia). This model was used to predict time to 50% hatching (ET_{50}). Coefficients, standard errors; and p-values are shown for each predictor.

Parameters (GLM)	*Coefficients*	*Std. Error*	*z-value*	*p-value*
(Intercept)	-25.7312	0.8701	-29.5740	< 0.0001 ***
O_2(12.5%)	1.8225	0.4239	4.2990	0.00002 ***
O_2(25%)	2.3436	0.4959	4.7260	< 0.0001 ***
O_2(50%)	1.8628	0.4155	4.4840	0.00001 ***
O_2(200%)	-0.1948	0.3792	-0.5140	0.60748
Temp(15.7°C)	-10.1363	1.4748	-6.8730	< 0.0001 ***
Temp(18.1°C)	-6.3693	0.4250	-14.9880	< 0.0001 ***
Temp(20.3°C)	-4.6328	0.4008	-11.5590	< 0.0001 ***
Temp(22.5°C)	-1.9670	0.3799	-5.1780	< 0.0001 ***
Temp(25.2°C)	0.5331	0.4179	1.2760	0.20201
Temp(29.4°C)	0.8488	0.4150	2.0450	0.04083 *
Temp(32°C)	3.6409	0.5222	6.9720	< 0.0001 ***
Temp(35.6°C)	3.5634	0.4647	7.6690	< 0.0001 ***
Temp(39.3°C)	0.2245	1.5849	0.1420	0.88736
O_2(12.5%):Temp(15.7°C)	-2.5674	2.0789	-1.2350	0.21685
O_2(25%):Temp(15.7°C)	-2.8680	2.0989	-1.3660	0.17181
O_2(50%):Temp(15.7°C)	-2.3014	2.0830	-1.1050	0.26922
O_2(200%):Temp(15.7°C)	0.0693	2.0836	0.0330	0.97346
O_2(12.5%):Temp(18.1°C)	-2.9697	0.6200	-4.7900	< 0.0001 ***
O_2(25%):Temp(18.1°C)	-3.5675	0.6918	-5.1570	< 0.0001 ***

O_2(50%):Temp(18.1°C)	-6.1542	1.5286	-4.0260	0.00006 ***
O_2(200%):Temp(18.1°C)	-1.6456	0.6608	-2.4900	0.01276 *
O_2(12.5%):Temp(20.3°C)	-0.1308	0.5530	-0.2360	0.81305
O_2(25%):Temp(20.3°C)	-1.3390	0.6145	-2.1790	0.02933 *
O_2(50%):Temp(20.3°C)	-2.9215	0.5863	-4.9830	< 0.0001 ***
O_2(200%):Temp(20.3°C)	0.9848	0.5353	1.8400	0.06582
O_2(12.5%):Temp(22.5°C)	-1.9238	0.5487	-3.5060	0.00045 ***
O_2(25%):Temp(22.5°C)	-1.0966	0.6247	-1.7550	0.07917 *
O_2(50%):Temp(22.5°C)	-1.7295	0.5650	-3.0610	0.0022 **
O_2(200%):Temp(22.5°C)	-0.5116	0.5226	-0.9790	0.32755
O_2(12.5%):Temp(25.2°C)	-2.2347	0.6123	-3.6500	0.00026 ***
O_2(25%):Temp(25.2°C)	-1.2161	0.6700	-1.8150	0.0695 ·
O_2(50%):Temp(25.2°C)	-2.7798	0.6009	-4.6260	< 0.0001 ***
O_2(200%):Temp(25.2°C)	-1.1439	0.5702	-2.0060	0.04485 *
O_2(12.5%):Temp(29.4°C)	-3.8866	0.5854	-6.6400	< 0.0001 ***
O_2(25%):Temp(29.4°C)	-2.0495	0.6520	-3.1430	0.00167 **
O_2(50%):Temp(29.4°C)	-0.5201	0.6403	-0.8120	0.41659
O_2(200%):Temp(29.4°C)	-1.1690	0.5560	-2.1030	0.03549 *
O_2(12.5%):Temp(32°C)	-13.1201	1.5821	-8.2930	< 0.0001 ***
O_2(25%):Temp(32°C)	-6.0797	0.7280	-8.3510	< 0.0001 ***
O_2(50%):Temp(32°C)	-2.4667	0.7134	-3.4580	0.00055 ***
O_2(200%):Temp(32°C)	-0.6064	0.7152	-0.8480	0.39656
O_2(12.5%):Temp(35.6°C)	-11.1369	1.5641	-7.1200	< 0.0001 ***
O_2(25%):Temp(35.6°C)	-11.7437	1.5839	-7.4140	< 0.0001 ***
O_2(50%):Temp(35.6°C)	-5.9753	0.6571	-9.0940	< 0.0001 ***
O_2(200%):Temp(35.6°C)	-4.4209	0.5949	-7.4310	< 0.0001 ***
O_2(12.5%):Temp(39.3°C)	0.4634	2.2625	0.2050	0.83770
O_2(25%):Temp(39.3°C)	-0.8111	2.2380	-0.3620	0.71705
O_2(50%):Temp(39.3°C)	-0.2005	2.2286	-0.0900	0.92833
O_2(200%):Temp(39.3°C)	2.0225	2.2341	0.9050	0.36531
log(hpf)	5.9284	0.1870	31.7010	< 0.0001 ***

Null deviance:	6068.18 on 563 degrees of freedom
Residual deviance:	530.22 on 513 degrees of freedom
AIC:	1078.4
Number of Fisher Scoring iterations:	10

Table S6: Effect of oxygen, temperature, and developmental time on hatching success in *Experiment 2*. GLM includes oxygen level, temperature centered to 27.8 °C ($Temp_1$, lowest temperature at which hatching occurred), and its quadratic term ($Temp_2$), their interaction, and log-transformed developmental time (hpf): Hatching success ~ O_2 + $Temp_1$ + $Temp_2$ + $O_2 \times Temp_1$ + $O_2 \times Temp_2$ + log(hpf) + (1 | Experiment). Significance is shown first with oxygen as numeric relative to 27.8 °C and subsequently relative to 100% air saturation. Estimates (β), standard errors, z-values, and p-values are shown for each predictor.

Parameters (GLM)	***Estimate (B)***	***Std. Error***	***z-value***	***p-value***
(Intercept)	-20.6800	0.4985	-41.4870	< 0.0001 ***
O_2	0.0062	0.0010	6.1460	< 0.0001 ***
$Temp_1$	0.6726	0.0675	9.9660	< 0.0001 ***
$Temp_2$	-0.1184	0.0088	-13.4460	< 0.0001 ***
O_2:$Temp_1$	0.0024	0.0006	4.0030	0.0001 ***
O_2:$Temp_2$	-0.0002	0.0001	-3.1210	0.0018 **
log(hpf)	4.7390	0.1118	42.3990	< 0.0001 ***
Null deviance:	7709.4 on 399 degrees of freedom			
Residual deviance:	2362.9 on 393 degrees of freedom			
AIC:	2885.1			
Num.Fisher Scoring iterations:	3			
Parameters (GLM)	***Estimate (B)***	***Std. Error***	***z-value***	***p-value***
(Intercept)	-24.5700	0.6418	-38.278	< 0.0001 ***
O_2(12.5%)	-3.5550	0.2641	-13.462	< 0.0001 ***
O_2(25%)	0.4599	0.2571	1.789	0.0737 ·
O_2(50%)	0.3232	0.2562	1.262	0.2071
O_2(200%)	-0.0464	0.2430	-0.191	0.8486
$Temp_1$	1.2810	0.1000	12.819	< 0.0001 ***
$Temp_2$	-0.1703	0.0110	-15.494	< 0.0001 ***

O_2(12.5%):$Temp_1$	0.1941	0.1728	1.123	0.2615
O_2(25%):$Temp_1$	-0.5149	0.1744	-2.953	0.0032 **
O_2(50%):$Temp_1$	-0.1122	0.1434	-0.783	0.4338
O_2(200%):$Temp_1$	-0.1242	0.1340	-0.927	0.3541
O_2(12.5%):$Temp_2$	-0.0623	0.0247	-2.517	0.0118 *
O_2(25%):$Temp_2$	-0.0389	0.0251	-1.552	0.1208
O_2(50%):$Temp_2$	0.0016	0.0163	0.100	0.9201
O_2(200%):$Temp_2$	0.0003	0.0148	0.021	0.9836
log(hpf)	5.8840	0.1459	40.318	< 0.0001 ***
Null deviance:	7709.4 on 399 degrees of freedom			
Residual deviance:	1179.7 on 384 degrees of freedom			
AIC:	1720			
Num.Fisher Scoring iterations:	3			

Table S7: Effect of oxygen, temperature, and developmental time on hatching success in *Experiment 2*. Effect of oxygen level, temperature, and time post-fertilization (hpf) on hatching success of *Danio rerio* embryos, derived from a GLM: Hatching success ~ O_2 × Temp + log(hpf). Post hoc comparisons were conducted relative to the control treatment (27.8 °C, normoxia). This model was used to predict time to 50% hatching (ET_{50}). Coefficients, standard errors; and p-values are shown for each predictor.

Parameters (GLM)	***Coefficients***	***Std. Error***	***z-value***	***p-value***
(Intercept)	-25.4008	0.6992	-36.3270	< 0.0001 ***
O_2(12.5%)	-3.2721	0.3293	-9.9370	< 0.0001 ***
O_2(25%)	0.1484	0.3442	0.4310	0.66629
O_2(50%)	-0.5093	0.3468	-1.4680	0.14201
O_2(200%)	-0.3443	0.3308	-1.0410	0.29791
Temp(28.4°C)	-0.3710	0.3862	-0.9610	0.33670
Temp(29.5°C)	1.0031	0.3624	2.7680	0.00564 **
Temp(30.4°C)	0.3344	0.3626	0.9220	0.35641
Temp(31.4°C)	1.2272	0.3662	3.3510	0.00081 ***
Temp(32.4°C)	2.1239	0.3832	5.5420	< 0.0001 ***

Temp(33.3°C)	1.2181	0.3671	3.3180	0.00091
Temp(34.5°C)	0.5842	0.3549	1.6460	0.09977
Temp(35.8°C)	0.9323	0.3830	2.4340	0.01493 *
Temp(37.1°C)	-7.9833	1.4600	-5.4680	< 0.0001 ***
O_2(12.5%):Temp(28.4°C)	-1.6848	0.5401	-3.1190	0.00181 **
O_2(25%):Temp(28.4°C)	0.4760	0.5169	0.9210	0.35713
O_2(50%):Temp(28.4°C)	1.5334	0.5315	2.8850	0.00392 **
O_2(200%):Temp(28.4°C)	0.4480	0.5090	0.8800	0.37872
O_2(12.5%):Temp(29.5°C)	-0.4888	0.4711	-1.0380	0.29939
O_2(25%):Temp(29.5°C)	-1.8470	0.5152	-3.5850	0.00034 ***
O_2(50%):Temp(29.5°C)	1.1248	0.5244	2.1450	0.03197 *
O_2(200%):Temp(29.5°C)	-0.0036	0.4935	-0.0070	0.99413
O_2(12.5%):Temp(30.4°C)	1.9022	0.5050	3.7670	0.00017 ***
O_2(25%):Temp(30.4°C)	-0.0434	0.5102	-0.0850	0.93224
O_2(50%):Temp(30.4°C)	1.5466	0.5309	2.9130	0.00358 **
O_2(200%):Temp(30.4°C)	0.4625	0.4982	0.9280	0.35330
O_2(12.5%):Temp(31.4°C)	-0.5664	0.4818	-1.1760	0.23969
O_2(25%):Temp(31.4°C)	-1.5425	0.5149	-2.9960	0.00274 **
O_2(50%):Temp(31.4°C)	0.0625	0.5257	0.1190	0.90530
O_2(200%):Temp(31.4°C)	1.0027	0.5157	1.9440	0.05188 ·
O_2(12.5%):Temp(32.4°C)	-1.0782	0.5292	-2.0370	0.04161 *
O_2(25%):Temp(32.4°C)	-3.1643	0.5166	-6.1250	< 0.0001 ***
O_2(50%):Temp(32.4°C)	-0.2523	0.5239	-0.4820	0.63008
O_2(200%):Temp(32.4°C)	-1.2446	0.5091	-2.4450	0.01449 *
O_2(12.5%):Temp(33.3°C)	0.9698	0.5179	1.8730	0.0611 ·
O_2(25%):Temp(33.3°C)	-3.3581	0.5010	-6.7030	< 0.0001 ***
O_2(50%):Temp(33.3°C)	-0.1684	0.5317	-0.3170	0.75145
O_2(200%):Temp(33.3°C)	-0.3551	0.5038	-0.7050	0.48083
O_2(12.5%):Temp(34.5°C)	-5.4563	1.4939	-3.6520	0.00026 ***
O_2(25%):Temp(34.5°C)	-8.2046	1.4996	-5.4710	< 0.0001 ***
O_2(50%):Temp(34.5°C)	1.3427	0.5216	2.5740	0.01005 *

O_2(200%):Temp(34.5°C)	-0.4701	0.4916	-0.9560	0.33898
O_2(12.5%):Temp(35.8°C)	-3.9199	1.5096	-2.5970	0.00941 **
O_2(25%):Temp(35.8°C)	-8.5087	1.5078	-5.6430	< 0.0001 ***
O_2(50%):Temp(35.8°C)	-2.1024	0.6062	-3.4680	0.00052 ***
O_2(200%):Temp(35.8°C)	-2.2404	0.5046	-4.4400	< 0.0001 ***
O_2(12.5%):Temp(37.1°C)	5.3383	2.0750	2.5730	0.01009 *
O_2(25%):Temp(37.1°C)	1.5752	2.0675	0.7620	0.44611
O_2(50%):Temp(37.1°C)	1.8417	2.0785	0.8860	0.37559
O_2(200%):Temp(37.1°C)	0.0890	2.0571	0.0430	0.96548
log(hpf)	6.2491	0.1590	39.3090	< 0.0001 ***
Null deviance:	7620.39 on 399 degrees of freedom			
Residual deviance:	711.17 on 349 degrees of freedom			
AIC:	1321.4			
Num.Fisher Scoring iterations:	5			

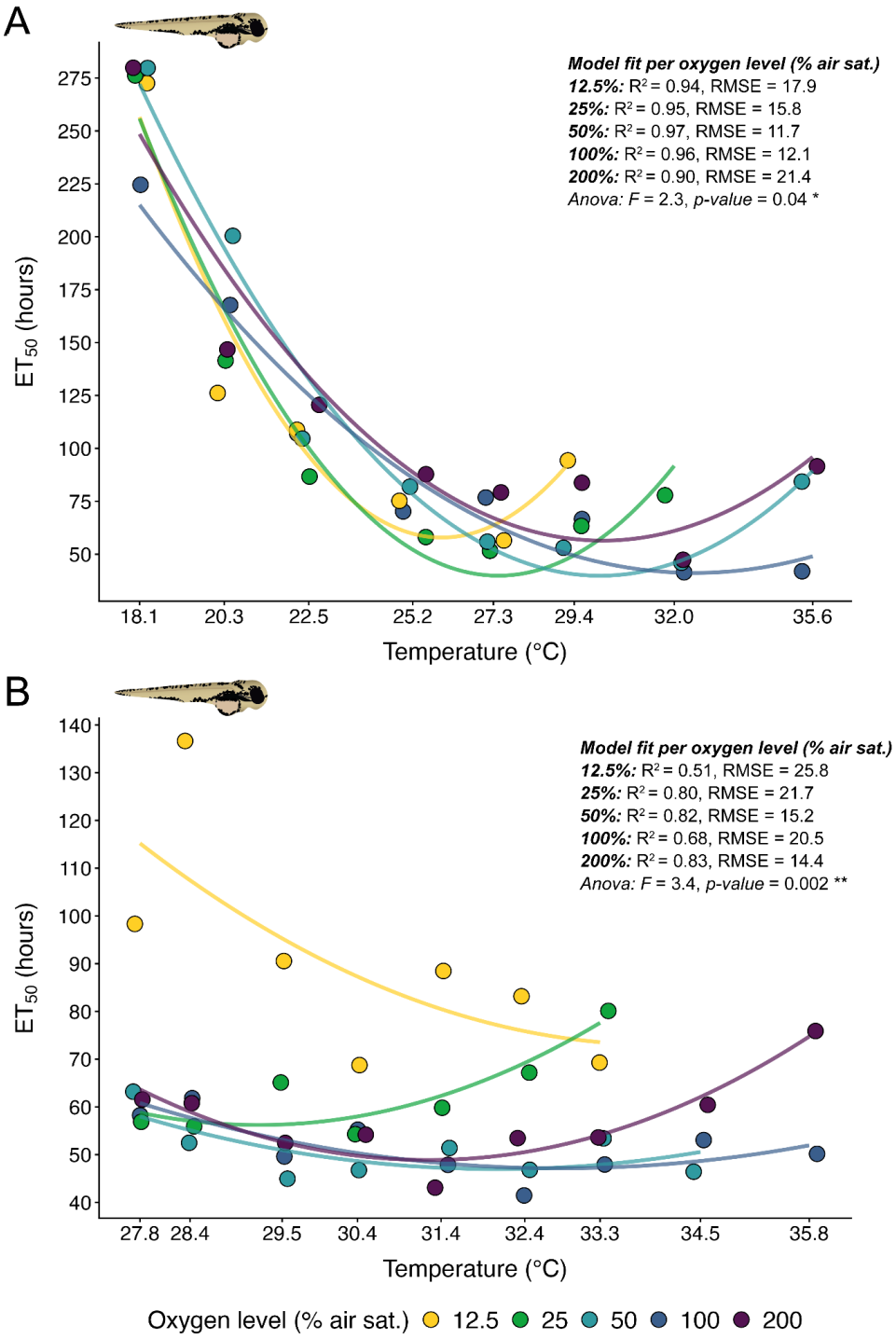

Fig. S9: Model-predicted time to 50% hatching (ET_{50}) in zebrafish (*Danio rerio*). Predicted ET_{50} (hours) for (A) *Experiment 1* and (B) *Experiment 2* based on GLM: Hatching success ~ Oxygen × Temperature + log(hpf) (Table S5-S7). Oxygen and temperature were included as factors, and hours post-fertilization (hpf) were log-transformed. The models achieved best-fit AIC values. Colored lines represent predicted 50% hatching times for each oxygen level fitted with a second-order polynomial regression (Predicted ET_{50} ~ poly(Temperature, 2)). Coefficients of determination (R^2) and root-mean-square deviation (RMSE) indicate regression fit quality per oxygen level. P-values denote significant effects of oxygen treatment on the temperature–hatching time relationship.

Table S8: Predicted time to 50% hatching (ET_{50} ; hours) for each combination of oxygen level and temperature treatment in *Danio rerio* from *Experiments 1* and *2*. Predictions were derived from a GLM: Hatching success ~ Oxygen × Temperature + log(hpf) (Table S5-S7), used to generate Fig. S8.

Experiment 1			Experiment 2		
Temperature (°C)	Oxygen (% air sat)	Predicted ET_{50}	Temperature (°C)	Oxygen (% air sat)	Predicted ET_{50}
15.7	12.5	–	27.8	12.5	98.33
18.1	12.5	272.66	28.4	12.5	136.65
20.3	12.5	126.03	29.5	12.5	90.54
22.5	12.5	108.76	30.4	12.5	68.75
25.2	12.5	75.18	31.4	12.5	88.47
27.3	12.5	56.43	32.4	12.5	83.17
29.4	12.5	94.18	33.3	12.5	69.27
32.0	12.5	–	34.5	12.5	–
35.6	12.5	–	35.8	12.5	–
39.3	12.5	–	37.1	12.5	–
15.7	25	–	27.8	25	56.88
18.1	25	276.24	28.4	25	55.93
20.3	25	141.51	29.5	25	65.10
22.5	25	86.63	30.4	25	54.29
25.2	25	57.99	31.4	25	59.82
27.3	25	51.67	32.4	25	67.18
29.4	25	63.28	33.3	25	80.11
32.0	25	77.97	34.5	25	–
35.6	25	–	35.8	25	–
39.3	25	–	37.1	25	–
15.7	50	–	27.8	50	63.19
18.1	50	279.83	28.4	50	52.48
20.3	50	200.39	29.5	50	44.95
22.5	50	104.56	30.4	50	46.76
25.2	50	81.87	31.4	50	51.40

27.3	50	56.04	32.4	50	46.83
29.4	50	53.02	33.3	50	53.41
32.0	50	45.98	34.5	50	46.43
35.6	50	84.18	35.8	50	–
39.3	50	–	37.1	50	–
15.7	100	–	27.8	100	58.26
18.1	100	224.71	28.4	100	61.82
20.3	100	167.61	29.5	100	49.61
22.5	100	106.94	30.4	100	55.21
25.2	100	70.12	31.4	100	47.86
27.3	100	76.72	32.4	100	41.46
29.4	100	66.49	33.3	100	47.93
32.0	100	41.52	34.5	100	53.05
35.6	100	42.07	35.8	100	50.17
39.3	100	–	37.1	100	–
15.7	200	–	27.8	200	61.55
18.1	200	279.83	28.4	200	60.80
20.3	200	146.73	29.5	200	52.45
22.5	200	120.45	30.4	200	54.19
25.2	200	87.88	31.4	200	43.08
27.3	200	79.30	32.4	200	53.46
29.4	200	83.68	33.3	200	53.61
32.0	200	47.52	34.5	200	60.43
35.6	200	91.64	35.8	200	75.88
39.3	200	–	37.1	200	–

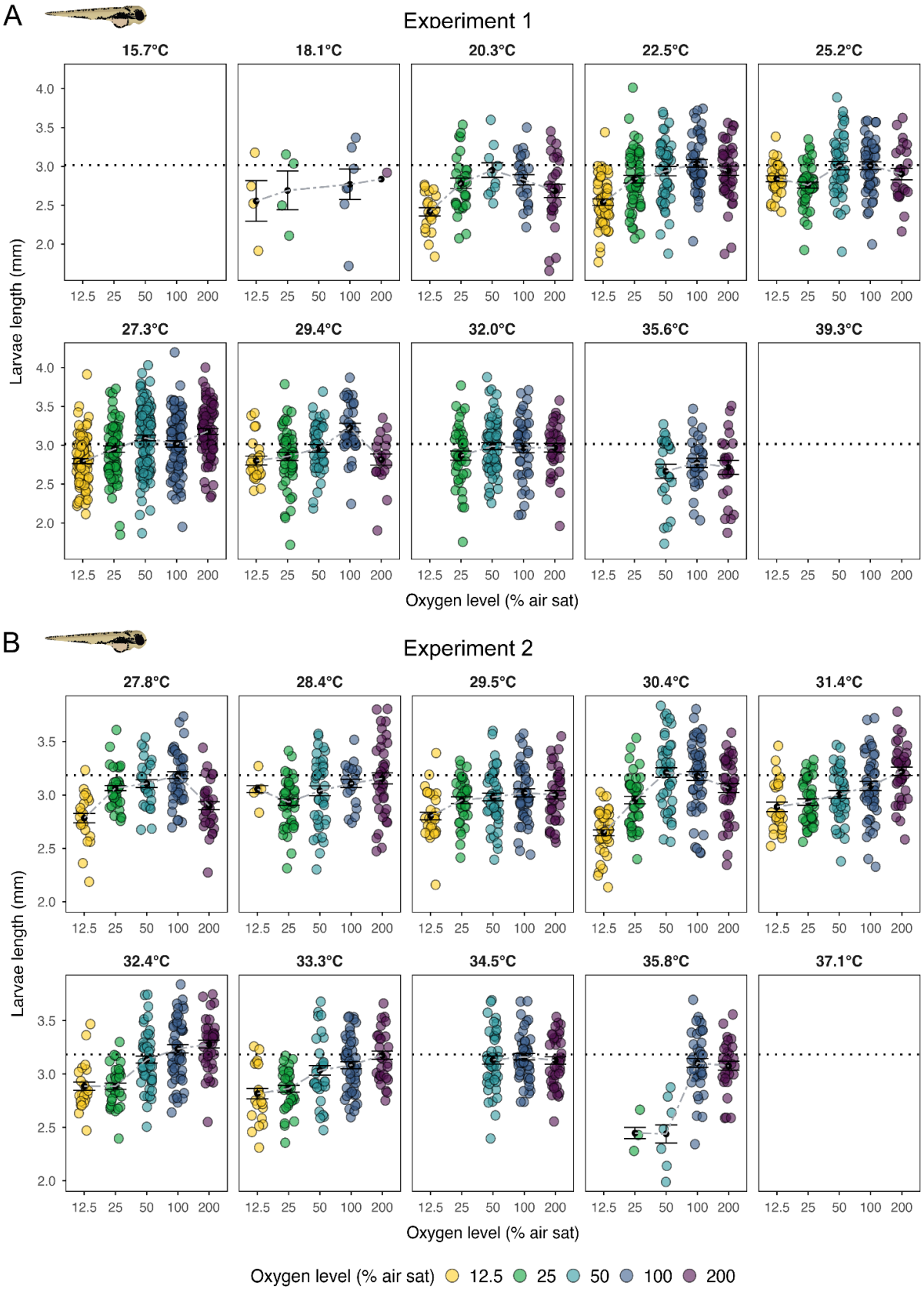

Fig. S10: Larval length (mm) of zebrafish (*Danio rerio*) across oxygen levels (colors) and temperatures (panel columns) in *Experiment 1* (n = 2–15; A) **and *Experiment 2*** (n = 2–24; B). Points show individual larvae (jittered); black circles and dashed lines indicate group

means ± S.E. Dotted lines mark control means (*Exp 1*: 27.3 °C, normoxia = 3.0 mm; *Exp 2*: 27.8 °C, normoxia = 3.2 mm).

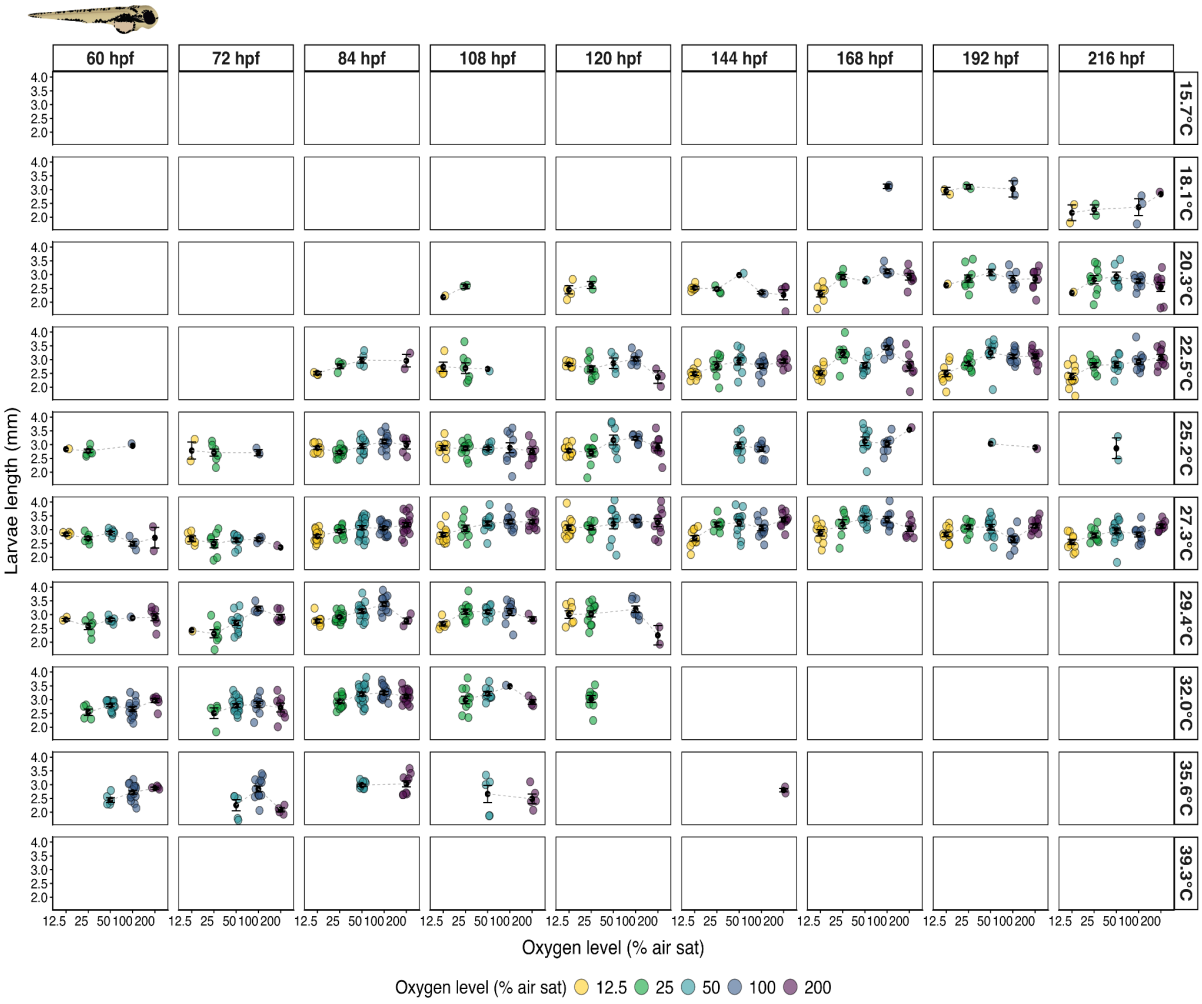

Figure S11 | Larval length of zebrafish across temperature, oxygen, and developmental time in *Experiment 1*. Larval length (mm) of *Danio rerio* across oxygen levels (colors) and temperatures (vertical panels) over time post-fertilization (60, 72, 84, 120, 144, 168, 192, and 216 hpf; horizontal panels). Points represent individual larvae; black circles indicate group means ± s.e., and grey dashed lines connect mean values across developmental time.

Table S9: Larval length of zebrafish across temperature, oxygen, and developmental time in *Experiment 1*. Anova (type III) and linear model (LM) includes oxygen level, temperature centered to 15.7 °C ($Temp_1$), and its quadratic term ($Temp_2$), their interaction, and developmental time (hpf): Length ~ O_2 + $Temp_1$ + $Temp_2$ + O_2×$Temp_1$ + O_2×$Temp_2$ + hpf. Significance was assessed relative to 15.7 °C and 100% air saturation. Estimates (β), standard errors (SE), t-values, and p-values are shown for each predictor.

Parameters (Anova, type III)	*Sum Squares*	*Df*	*F-value*	*p-value*
(Intercept)	96.714	1	747.933	< 0.0001 ***
O_2	1.662	4	3.212	0.0123*

$Temp_1$	3.114	1	24.081	< 0.0001 ***
$Temp_2$	3.004	1	23.232	< 0.0001 ***
O_2:$Temp_1$	1.129	4	2.183	0.0687
O_2:$Temp_2$	1.047	4	2.025	0.0886
hpf	1.888	1	14.601	0.00014***
Residuals	185.041	1431		

Parameters (LM)	***Estimate (B)***	***Std. Error***	***t-value***	***p-value***
(Intercept)	2.533	0.093	27.348	< 0.0001 ***
O_2(12.5%)	-0.423	0.139	-3.042	0.0024**
O_2(25%)	-0.023	0.116	-0.203	0.8394
O_2(50%)	-0.074	0.135	-0.550	0.5822
O_2(200%)	-0.250	0.117	-2.140	0.0325*
$Temp_1$	0.085	0.017	4.907	< 0.0001 ***
$Temp_2$	-0.004	0.001	-4.820	< 0.0001 ***
hpf	0.001	0.000	3.821	0.0001***
O_2(12.5%):$Temp_1$	0.007	0.043	0.161	0.8717
O_2(25%):$Temp_1$	-0.037	0.029	-1.273	0.2032
O_2(50%):$Temp_1$	0.017	0.028	0.605	0.5452
O_2(200%):$Temp_1$	0.052	0.026	1.963	0.0498*
O_2(12.5%):$Temp_2$	0.001	0.003	0.305	0.7603
O_2(25%):$Temp_2$	0.002	0.002	1.273	0.2033
O_2(50%):$Temp_2$	-0.001	0.001	-0.771	0.4406
O_2(200%):$Temp_2$	-0.003	0.001	-1.889	0.0591

Residual standard error:	0.3596 on 1431 degrees of freedom
Multiple R-squared:	0.154
F-statistic:	17.37 on 15 and 1431 DF, p-value: < 0.0001 ***
Adjusted R-squared:	0.1452

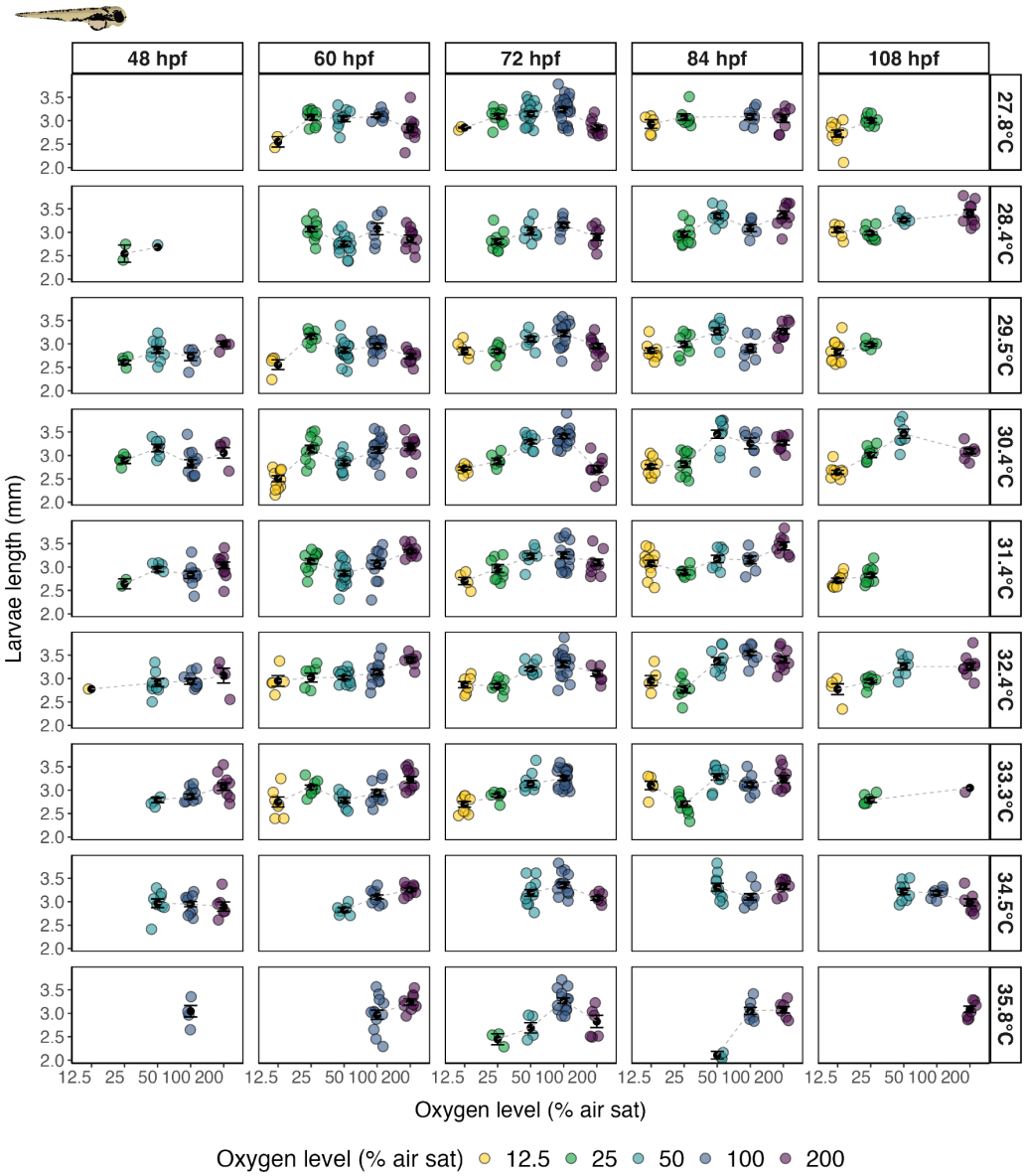

Fig. S12: Larval length of zebrafish across temperature, oxygen, and developmental time in *Experiment 2.* Larval length (mm) of *Danio rerio* across oxygen levels (colors) and temperatures (vertical panels) over time post-fertilization (48, 60, 72, 84, and 108 hpf; horizontal panels). Points represent individual larvae; black circles indicate group means ± s.e., and grey dashed lines connect mean values across developmental time.

Table S10: Larval length of zebrafish across temperature, oxygen, and developmental time in *Experiment 2.* Anova (type III) and linear model (LM) includes oxygen level, temperature centered to 27.8 °C ($Temp_1$), and its quadratic term ($Temp_2$), their interaction, and developmental time (hpf): Length ~ O_2 + $Temp_1$ + $Temp_2$ + O_2×$Temp_1$ + O_2×$Temp_2$ + hpf. Significance was assessed relative to 27.8 °C and 100% air saturation. Estimates (β), standard errors (SE), t-values, and p-values are shown for each predictor.

Parameters (Anova, type III)	*Sum Squares*	*Df*	*F-value*	*p-value*
(Intercept)	262.798	1	3991.617	< 0.0001 ***

O_2	3.127	4	11.874	< 0.0001 ***
$Temp_1$	0.039	1	0.597	0.4398
$Temp_2$	0.037	1	0.556	0.4560
O_2:$Temp_1$	1.466	4	5.566	0.0002***
O_2:$Temp_2$	1.258	4	4.776	0.0008***
hpf	7.414	1	112.605	< 0.0001 ***
Residuals	92.699	1408		

Parameters (LM)	***Estimate (B)***	***Std. Error***	***t-value***	***p-value***
(Intercept)	2.809	0.044	63.179	< 0.0001 ***
O_2(12.5%)	-0.410	0.062	-6.577	< 0.0001 ***
O_2(25%)	-0.166	0.046	-3.586	0.0003***
O_2(50%)	-0.112	0.048	-2.332	0.0198*
O_2(200%)	-0.193	0.047	-4.077	< 0.0001 ***
$Temp_1$	0.014	0.019	0.773	0.4398
$Temp_2$	-0.002	0.002	-0.746	0.4560
hpf	0.004	0.000	10.612	< 0.0001 ***
O_2(12.5%):$Temp_1$	-0.051	0.044	-1.148	0.2512
O_2(25%):$Temp_1$	-0.013	0.031	-0.429	0.6682
O_2(50%):$Temp_1$	0.056	0.029	1.916	0.0555
O_2(200%):$Temp_1$	0.099	0.028	3.579	0.0004***
O_2(12.5%):$Temp_2$	0.013	0.007	1.835	0.0667
O_2(25%):$Temp_2$	-0.004	0.005	-0.857	0.3917
O_2(50%):$Temp_2$	-0.009	0.004	-2.460	0.0139*
O_2(200%):$Temp_2$	-0.011	0.003	-3.154	0.0016**

Residual standard error:	0.2566 on 1408 degrees of freedom
Multiple R-squared:	0.2336
F-statistic:	28.61 on 15 and 1408 DF, p-value: < 0.0001 ***
Adjusted R-squared:	0.2255

Table S11: Survival to first feeding of zebrafish across temperature, oxygen, and developmental time in *Experiment 1 and 2.* GLM-TMB includes oxygen level, temperature

centered to 18.1 °C ($Temp_1$, lowest temperature at which hatching occurred), and its quadratic term ($Temp_2$), their interaction, log-transformed developmental time (hpf), and Experiment as random effect: Survival to First Feeding ~ O_2 + $Temp_1$ + $Temp_2$ + O_2×$Temp_1$ + O_2×$Temp_2$ + log(hpf) + (1 | Experiment). Significance is shown first with oxygen as numeric relative to 18.1 °C and subsequently relative to 100% air saturation. Estimates (β), standard errors (SE), z-values, and p-values are shown for each predictor.

Parameters (GLM-TMB)	***Estimate (B)***	***Std. Error***	***z-value***	***p-value***
(Intercept)	-26.1100	0.5732	-45.550	< 0.0001 ***
O_2	-0.0114	0.0022	-5.180	< 0.0001 ***
$Temp_1$	0.9085	0.0391	23.230	< 0.0001 ***
$Temp_2$	-0.0433	0.0019	-22.370	< 0.0001 ***
O_2:$Temp_1$	0.0028	0.0004	7.020	< 0.0001 ***
O_2:$Temp_2$	-0.0001	0.0000	-5.500	< 0.0001 ***
log(hpf)	4.6060	0.0990	46.510	< 0.0001 ***
Experiment (Intercept):	0.0598 (Var.)	0.2446 (St. Dev.)		
Number of obs:	973	groups:	Experiment 1, 2	
AIC:	6960.7	logLik:	-3472.3	

Parameters (GLM-TMB)	***Estimate (B)***	***Std. Error***	***z-value***	***p-value***
(Intercept)	-38.6488	0.8895	-43.450	< 0.0001 ***
O_2(12.5%)	-0.1135	0.4524	-0.250	0.8019
O_2(25%)	-1.8757	0.4954	-3.790	0.0001 ***
O_2(50%)	-4.9287	0.6807	-7.240	< 0.0001 ***
O_2(200%)	-2.4898	0.5497	-4.530	< 0.0001 ***
$Temp_1$	1.2624	0.0596	21.170	< 0.0001 ***
$Temp_2$	-0.0442	0.0026	-17.000	< 0.0001 ***
O_2(12.5%):$Temp_1$	0.1149	0.1301	0.880	0.3775
O_2(25%):$Temp_1$	1.1954	0.1088	10.980	< 0.0001 ***
O_2(50%):$Temp_1$	1.1965	0.1247	9.590	< 0.0001 ***
O_2(200%):$Temp_1$	0.6411	0.0995	6.440	< 0.0001 ***
O_2(12.5%):$Temp_2$	-0.0483	0.0091	-5.290	< 0.0001 ***
O_2(25%):$Temp_2$	-0.0919	0.0058	-15.870	< 0.0001 ***
O_2(50%):$Temp_2$	-0.0608	0.0055	-10.990	< 0.0001 ***

O_2(200%):$Temp_2$	-0.0394	0.0044	-9.000	< 0.0001 ***
log(hpf)	6.8743	0.1509	45.560	< 0.0001 ***
Experiment (Intercept):	0.08689 (Var.)	0.2948 (St. Dev.)		
Number of obs:	973	groups:	Experiment 1, 2	
AIC:	4348.5	logLik:	-2157.2	

Table S12: Larval count and survival of zebrafish transferred to control conditions. Number of larvae transferred to control conditions (28.0 ± 0.5 °C, normoxia) from *Experiment 1* and (27.0 ± 0.5 °C, normoxia) from *Experiment 2.* Hatched larvae that died during treatment exposure are indicated by †. Zero values denote treatments in which no hatching occurred.

		Oxygen level (% air sat)				
	Temperature (°C)	**12.5**	**25**	**50**	**100**	**200**
Experiment 1	**20.3**	8	10	4	9	9
	25.2	10	11	10	10	10
	29.4	2	11	9	10	8
	32	0	9	10	9	7
	35.6	0	0	†	13	1
Experiment 2	**27.8**	†	21	16	21	22
	29.5	†	13	20	20	22
	31.4	†	12	17	19	21
	33.3	†	3	15	19	19
	35.8	0	0	†	11	2

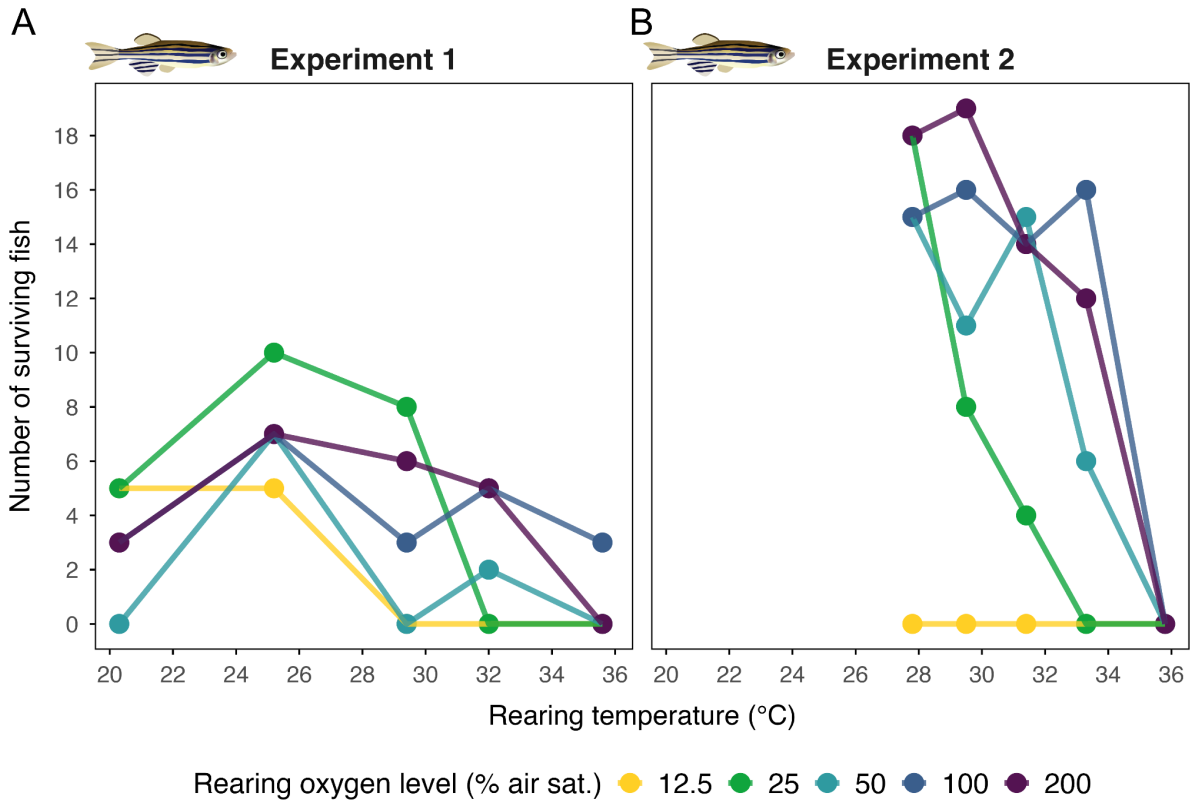

Fig. S13: Survival number of zebrafish reared across temperature and oxygen treatments. (A) Numbers represent individuals that survived to the juvenile stage after being transferred to control conditions from *Experiment 1* (normoxia; 28 °C) for CT_{max} testing during the juvenile stage. (B) equivalent data for *Experiment 2* (normoxia; 27 °C).

Table S13: Critical thermal maximum (CT_{max}) of zebrafish across rearing temperature and oxygen treatments in *Experiment 1.* Anova (type III) and linear model (LM) includes oxygen level (O_2), temperature (Temp), and their interaction: $CT_{max} \sim O_2 \times Temp$. Significance was assessed relative to 20.3 °C and 100% air saturation. Estimates (β), standard errors (SE), t-values, and p-values are shown for each predictor.

Parameters (Anova, type III)	Sum Squares	Df	F-value	P-value
O_2	0.747	4	1.717	0.1566
Temp	1.863	4	4.283	0.0038**
O_2:Temp	0.849	7	1.115	0.3644
Residuals	7.288	67		
Parameters (LM)	**Estimate (B)**	**Std. Error**	**t value**	**P-value**
(Intercept)	41.669	0.113	370.304	< 0.0001***
O_2(12.5%)	-0.304	0.138	-2.197	0.0311*
O_2(25%)	-0.022	0.109	-0.198	0.8439

O_2(50%)	-0.165	0.144	-1.147	0.2551
O_2(200%)	-0.134	0.107	-1.248	0.2160
Temp(20.5°C)	-0.324	0.122	-2.656	0.00967**
Temp(25.5°C)	-0.107	0.103	-1.042	0.3009
Temp(32°C)	0.156	0.133	1.170	0.2457
Temp(36°C)	-0.436	0.222	-1.962	0.05347·
Residual standard error:	0.3316 on 74 degrees of freedom			
Multiple R-squared:	0.2794			
F-statistic:	3.587 on 8 and 74 DF, p-value: 0.00144			
Adjusted R-squared:	0.2015			

Table S14: Critical thermal maximum (CT_{max}) of zebrafish across rearing temperature and oxygen treatments in *Experiment 2.* Anova (type III) and linear model (LM) includes oxygen level (O_2), temperature (Temp), and their interaction: $CT_{max} \sim O_2 \times Temp$. Significance was assessed relative to 27.8 °C and 100% air saturation. Estimates (β), standard errors (SE), t-values, and p-values are shown for each predictor.

Parameters (Anova, type III)	**Sum Squares**	**Df**	**F-value**	**P-value**
O_2	4.265	3	10.797	< 0.0001***
Temp	1.588	3	4.020	0.0084**
O_2:Temp	2.049	8	1.945	0.0559·
Residuals	24.097	183		
Parameters (LM)	**Estimate (B)**	**Std. Error**	**t value**	**P-value**
(Intercept)	40.808	0.065	629.348	< 0.0001***
O_2(25%)	-0.483	0.088	-5.490	< 0.0001***
O_2(50%)	-0.158	0.073	-2.163	0.0318*
O_2(200%)	-0.094	0.067	-1.407	0.1611
Temp(29.5°C)	0.115	0.069	1.657	0.0991
Temp(31.4°C)	0.025	0.072	0.340	0.7344
Temp(33.3°C)	-0.164	0.082	-2.014	0.0455*
Residual standard error:	0.37 on 191 degrees of freedom			
Multiple R-squared:	0.1714			

F-statistic:	6.583 on 6 and 191 DF, p-value: < 0.0001***
Adjusted R-squared:	0.1453

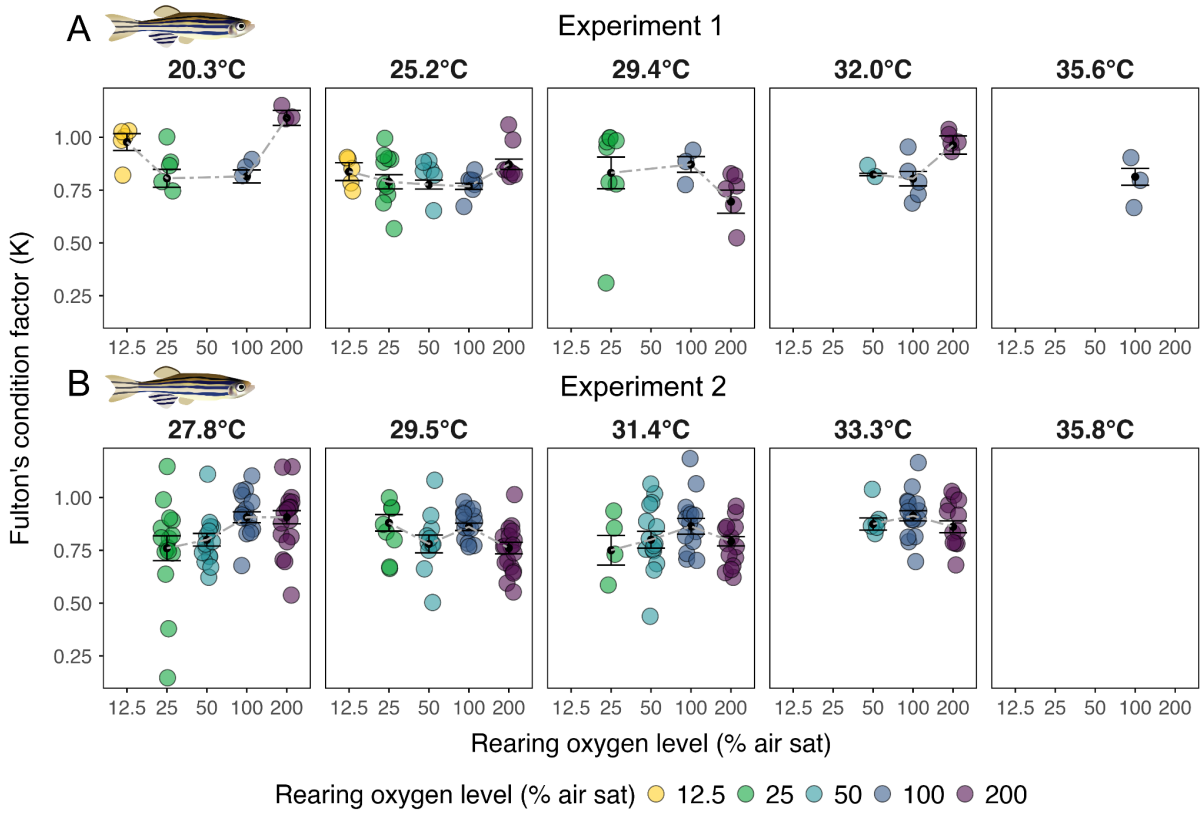

Fig. S14: Fulton's condition factor (K) of juvenile zebrafish across rearing temperature and oxygen treatments. Fulton's condition factor (K) of juvenile *Danio rerio* reared during the embryonic stage under five oxygen levels (colors) and temperature treatments (horizontal panels) in (A) *Experiment 1* and (B) *Experiment 2.* Points represent individual fish (jittered), with color indicating oxygen treatment.

Table S15: Fulton's condition factor (K) of juvenile zebrafish across rearing temperature and oxygen treatments for *Experiment 1* and *2*. Anova (type III) includes oxygen level (O_2) and temperature (Temp): K ~ O_2 + Temp. P-values are shown for each predictor.

Experiment 1

Parameters (Anova, type III)	*Sum Squares*	*Df*	*F-value*	*P-value*
(Intercept)	1.818	1	113.872	< 0.0001***
O_2	0.034	1	2.111	0.1502
Temp	0.052	1	3.237	0.0758
Residuals	1.277	80		

Experiment 2

Parameters (Anova, type III)	*Sum Squares*	*Df*	*F-value*	*P-value*
(Intercept)	0.417	1	22.120	< 0.0001***
O_2	0.012	1	0.635	0.4264
Temp	0.014	1	0.753	0.3868
Residuals	3.672	195		

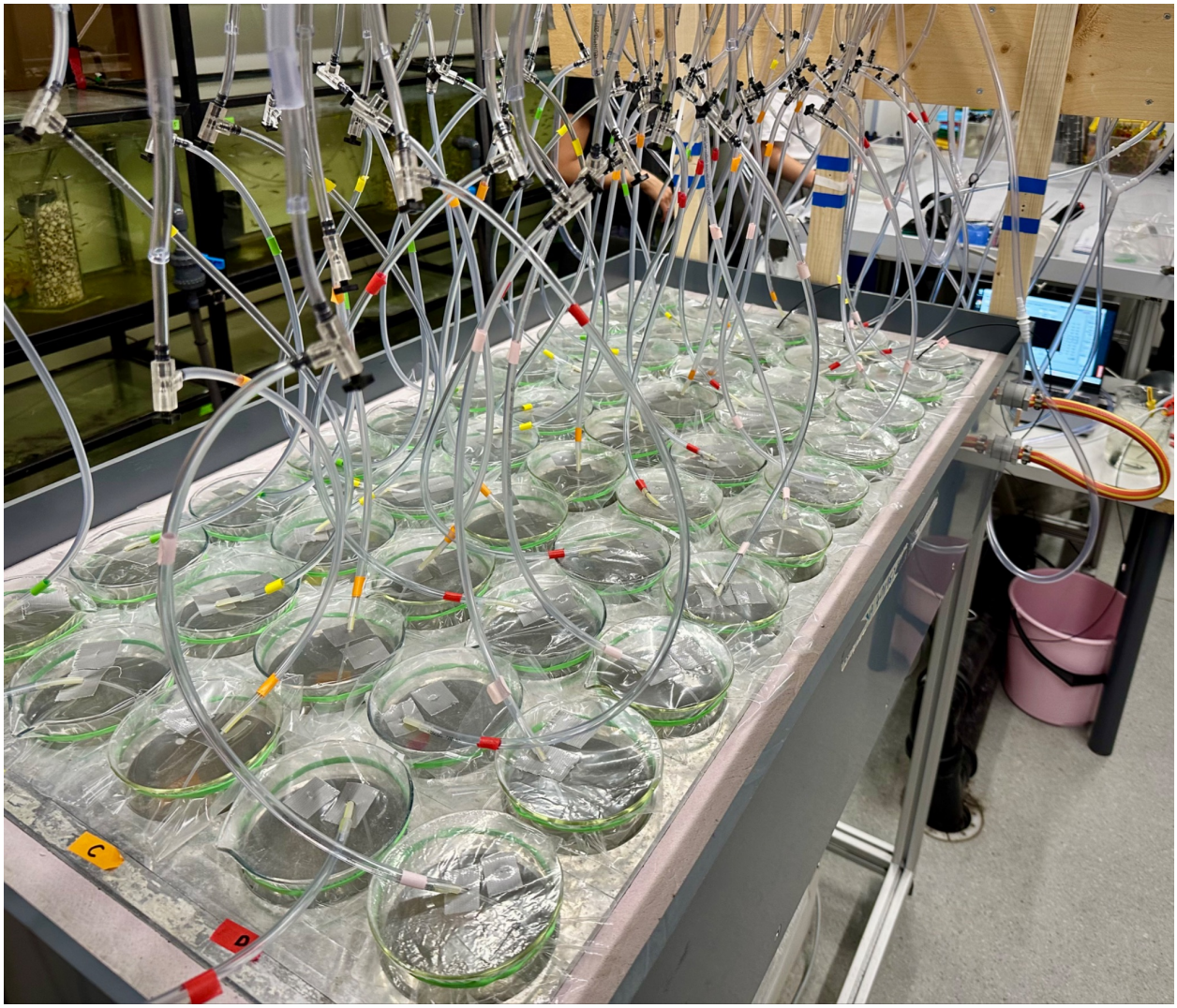

Fig. S15: Gradient table set up depicting a factorial design of 10 temperatures and 5 oxygen levels yielding 50 unique temperature-oxygen combinations. Color coded tubes supplied with air to each beaker, where different color lines represent an oxygen level. Beakers were hermetically covered to keep a constant DO_2 concentration per treatment. The mixed gas was delivered to the respective column of 10 beakers via a 10 mm diameter outflow tube. Each beaker was aerated through an individual air tube tightly inserted through the lid and fitted with an air valve, providing gentle bubbling.

Fig. S16: Beaker (800 mL) filled with 300 mL treated fresh water held the embryos and early larvae during the rearing period. The aluminium wells holding a beaker had a 17 cm depth.

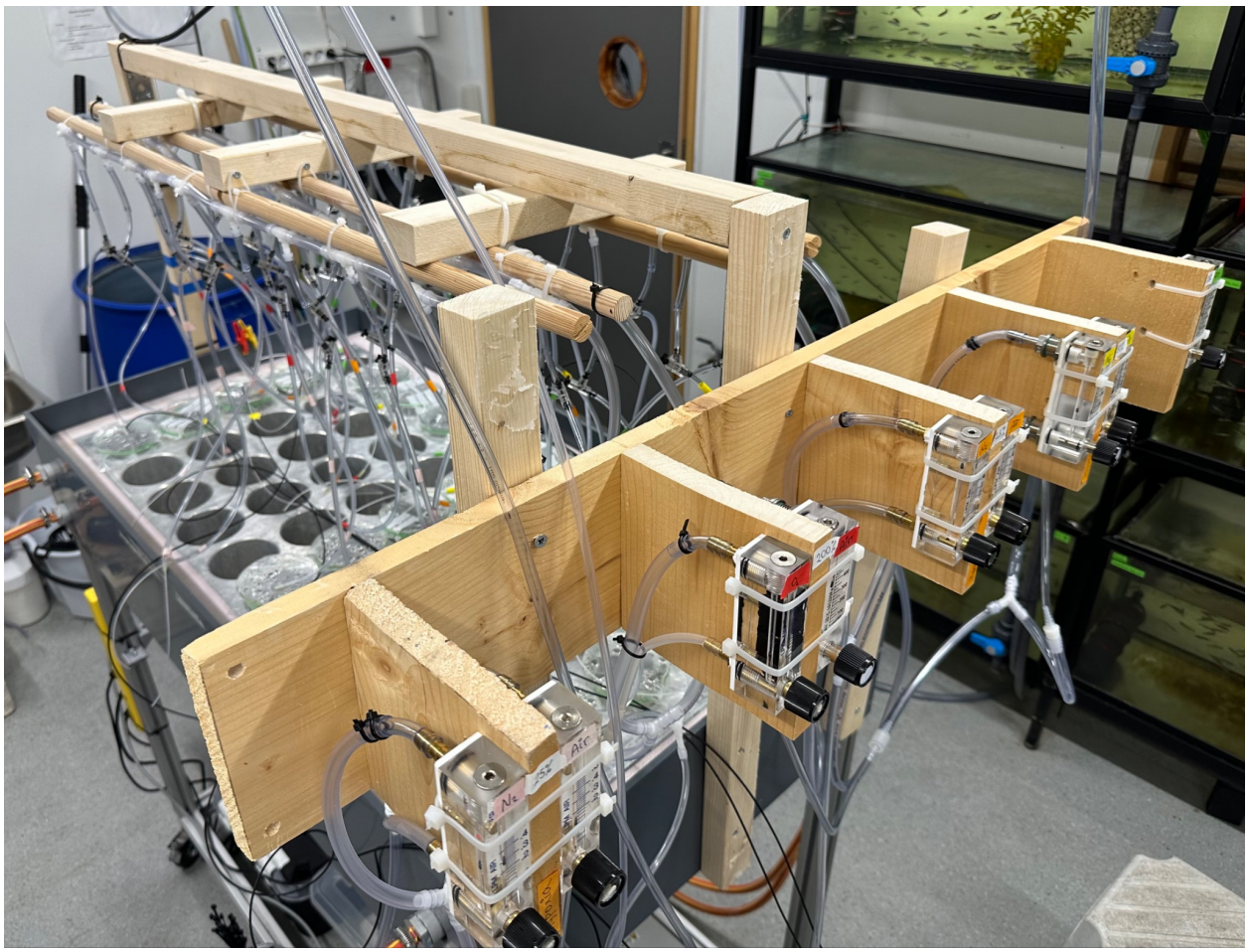

Fig. S17: Set up with five gas mixing stations per oxygen level (12.5, 25, 50, 100, and 200% air saturation). Oxygen concentrations were regulated using manual gas flow controllers (RS Pro, 500 ml/min) that mixed air with either nitrogen (50 L, 99.6% N2) or oxygen (50 L, 99.5% O2, Linde Co.) to create hypoxia or hyperoxia, respectively. Normoxia was achieved using ambient air. The two flow controllers supplied with the target oxygen concentration via a 10 mm diameter outflow tube to each column (10 beakers) of the thermal gradient table Each beaker was aerated through an individual air tube tightly inserted through the lid and fitted with an air valve, providing gentle bubbling.

Fig. S18: Aluminium gradient table connected to a cool and warm temperature water bath at each extreme. The system consisted of a cooler (Titan 200, Aqua Medic, Germany) and a heater circulator (Grant Instruments, GD100), each with a built-in thermostats that maintain their respective water baths at a set temperature. Water from each bath was pumped to the respective edges of the table using an Eheim Universal 1000 pump (Germany), generating a consistent thermal gradient, from cold to warm, across the aluminium slab of the table.